Phase transitions in ferromagnets with dipolar interactions and uniaxial anisotropy

K. Ried, Y. Millev,* M. Fähnle, and H. Kronmüller
Max-Planck-Institut für Metallforschung, Institut für Physik, Heisenbergstrasse 1, 70569 Stuttgart, Germany
(Received 29 August 1994)

A renormalized-field theory for the critical behavior of ferromagnets with dipolar interactions and uniaxial anisotropy is developed to the one-loop order whereby the (reduced) dipolar g and uniaxial m couplings are studied on equal footing. A generalized minimal subtraction scheme is used to study the attractors and the renormalized flow of the ϕ^4 coupling constant and, subsequently, to determine the Kouvel-Fisher effective exponent $\gamma_{\rm eff}$ for the longitudinal susceptibility for arbitrary values of m and g. Despite the difficulties brought about by the generality of treatment, the investigation was carried out analytically throughout. The crossover transitions between the four nontrivial fixed points (Heisenberg, Ising, uniaxial dipolar, and isotropic dipolar), as exemplified by $\gamma_{\rm eff}$, are determined in detail to the one-loop order of the theory. In particular, all previous predictions concerning the discussed features of criticality in dipolar ferromagnets are obtained as specific cases of the present study. The problems arising in an attempt to fix the physical scale in a renormalized-field theoretical treatment of crossover behavior are discussed in view of finding a quantitative interpretation of recent experimental results on Gd and $Fe_{14}Nd_2B$.

I. INTRODUCTION

The short-range exchange interaction is the dominant interaction in ferromagnetic materials and is responsible for the existence of spontaneous magnetization below a certain critical temperature. The theory of the second-order phase transition in magnetic materials with short-range exchange interactions is well established.[1–3] It turned out that the thermodynamic properties are governed by critical exponents which depend only on the number of components of the magnetization vector n and on the dimensionality of space d. In addition to the exchange interaction which is short ranged and isotropic, in real ferromagnets other physical interactions are present which differ in strength, range of action, and spatial symmetry. Outstanding examples are the dipolar interactions between the magnetic moments and the crystal-field interactions. The former are long ranged and are covariant (tensorial) rather than invariant (scalar) under spatial rotations while the latter induce anisotropy in the magnetic properties. While these interactions are typically one or two orders of magnitude smaller than the dominant exchange interaction, it is still a subject of current research how they influence the critical behavior of real ferromagnets.[4,5]

Below, we shall be interested in the modifications which arise in the critical behavior in the paramagnetic phase of ferromagnets with dominant exchange interaction, dipolar interaction between the ordering magnetic moments, and uniaxial anisotropy. As in almost all relevant studies on critical behavior in the presence of dipolar forces, our investigations are based on the fundamental work by Fisher and Aharony.[6,7] There they derived the proper Landau-Ginzburg-Wilson Hamiltonian for the renormalization-group (RG) treatment of the problem[8,9] in the presence of dipolar forces in a d-dimensional cubic system and gave a procedure for the estimation of the relevant parameters in terms of the respective material constants. Uniaxial anisotropy is incorporated into the analysis of the critical behavior along the lines set out in the phenomenological scaling theory of anisotropy[10] and developed later within the RG scheme.[11–13]

The *asymptotic* critical behavior of isotropic n-component ferromagnets in which dipolar effects are important has already been studied within the framework of the RG analysis and the ϵ expansion.[1,6,14] For XY ($n = 2$) and Heisenberg ($n = 3$) dipolar systems, the asymptotic behavior is governed by the dipolar fixed point of the RG recursion (flow) equations characterized by an infinite increase of the dipolar coupling constant. For the Heisenberg dipolar case, the values of most of the critical exponents are very close to those of the respective short-range model with a switched-off dipolar interaction.[15]

In contrast, for Ising ($n = 1$) dipolar systems, i.e., dipolar systems with infinite uniaxial anisotropy, the asymptotic behavior is characterized by mean-field exponents.[16–18] This drastic difference is directly related to the fact that the upper critical dimensionalities d_c, above which the corresponding mean-field description of criticality is exact, are different for Ising and non-Ising dipolar cases (d_c is 3 and 4, respectively[2]). Precisely at d_c, logarithmic corrections are expected[9] and, in fact, have been detected for the Ising dipolar system at $d_c = 3$ within the parquet-graph approximation[16] even before the advent of the RG analysis of phase transitions. This is the much-discussed mean-field behavior with logarithmic corrections. It must be emphasized that the effect of the dipolar interaction is different from that of a long-range exchange interaction.[19] There the critical behavior is driven towards the mean-field regime regardless of the value of n.

The account of *corrections* to the main scaling, i.e.,

asymptotic, behavior is inevitable in order to achieve a useful characterization of the experimentally accessible vicinity of the critical point. In the case of the dipolar ferromagnets in a nonasymptotic temperature region, the critical behavior characteristic for the respective short-range model shows up. Quite generally, the *crossover theory* explores the possibility for and the consequences of the switching over between different generic regimes of critical behavior upon variation of temperature. Theoretically, the different regimes of critical behavior belong to different fixed points of the RG transformation, as described by the corresponding universality classes which depend on underlying symmetries, range of interactions and dimensionalities of space, and order parameter field. Once the fixed points of the parameter flow under the action of the RG have been located, standard analysis of linear stability near the respective fixed points allows one to estimate, usually in an ϵ or $1/n$ expansion, the correction-to-scaling exponents as was demonstrated already in the pioneering papers on the subject.[8,11,20–22] Without further complications, one finds the crossover exponent which characterizes the way a system runs away to a new fixed point or, possibly, to infinity when further physically relevant perturbations are included into the problem and the "old" generic fixed point is no longer stable. In the above mentioned examples of isotropic dipolar ferromagnets the dipolar fixed point is stable and therefore determines the asymptotic critical behavior while the respective short-range fixed point is unstable and may influence the critical behavior in an intermediate-temperature region. If further perturbations, like anisotropies, are included, the number of possible fixed points increases and the critical behavior becomes more complicated, as will be shown below.

A fundamental difficulty which is then encountered within the RG perturbation expansion techniques is the sensitivity of the result to the initial (bare) values of the parameters. It is only when a given physical system evolves along a RG trajectory which traverses the immediate vicinity of one or more unstable generic fixed points that the critical behavior characteristic for the unstable attractors would show up. Consequently, the expected crossover between different regimes of critical behavior occurs only for a certain range of the initial values of the parameters. A further complication is that the "distance" of a given physical system to criticality in parameter space can be measured with reference to different fixed points. Early RG crossover treatments[23–27] exploited a reduced temperature variable referred, in the first instance, to the fixed point which becomes unstable under an additional perturbation; consequently, a matching condition has to be used to extend the analysis to the domain of attraction of the additional fixed point, that is, to the true asymptotic critical behavior whereby significant complications arise. As shown by Amit and Goldschmidt,[28] a more natural and advantageous crossover scheme can be formulated if the temperature scale is referred to the true asymptotic critical temperature from the very beginning. Below we extend this scheme to the more complex context of the present model.

It is the purpose of the present paper to study in detail the crossover in the critical behavior of ferromagnets with dipolar interactions and uniaxial anisotropy. We have chosen to characterize the crossover in the paramagnetic phase via the calculation of the effective temperature-dependent exponent γ_{eff} (Ref. 29) to the one-loop order of the renormalized-field theory:

$$\gamma_{\text{eff}} = \frac{\mathrm{d}\ln\chi_{11}^{-1}}{\mathrm{d}\ln\tau} \ . \tag{1}$$

Here χ_{11}^{-1} is the inverse longitudinal susceptibility, $\tau \sim (T - T_c)$, and T_c is the true critical temperature. The renormalization is carried out within the generalized minimal subtraction scheme[28] which is itself further generalized to match the more complicated situation encountered in the model discussed.

Different cases which will later be identified as particular cases of our investigation have already been studied. For instance, γ_{eff} for the crossover from short-range to dipolar critical behavior of Heisenberg ($n = 3$) ferromagnets exhibits a pronounced dip for reduced temperatures of the order of the reduced dipolar interaction.[26,27,30,31] This dip was claimed to be responsible for the experimentally observed susceptibility exponent in EuO and EuS.[32] For the crossover from short-range to dipolar critical behavior of Ising ($n = 1$) ferromagnets, γ_{eff} decreases from its short-range value γ_I to the asymptotical mean-field value of $\gamma = 1$.[33–35] This prediction complies with experiments on $LiTbF_4$.[34,36] Additionally, for ferromagnets without dipolar interactions, γ_{eff} has been calculated for different models which exhibit a crossover originating from the anisotropy of the short-range interaction.[23–25,28,37]

The substantial generalization and, hence, complication in the present study lie in the simultaneous analysis on equal footing of uniaxial anisotropy and dipolar forces as measured by their reduced coupling strengths m and g, respectively (see below). This introduces *two* additional characteristic lengths into the problem in the crossover region. The latter has therefore a structure which is far more complicated than in problems with a single additional characteristic length studied previously. The difficulties in tackling the two-scale problem were only partially overcome in a treatment in which the reduced coupling strengths m and g were set equal at a certain stage of the calculation, thus reducing it to an effectively single-scale one.[38] The results were related to experiments on $Fe_{14}Nd_2B$ (Ref. 39) via the additional plausible "mean-geometric" approximation $m = g \approx (m_{\text{expt}} g_{\text{expt}})^{1/2}$ and the experimental values under the square root were estimated from available experimental data.[40] A Brief Report on the results for general m and g focusing on the value of γ_{eff} with new nonuniversal logarithmic corrections as well as on some important intermediate results was given quite recently.[41] The generality of the procedures used and the results obtained allows their application to situations with any m and g relevant to experiments on such materials, including the known limiting

cases where one of the strengths is zero or infinitely large. Furthermore, the accomplishments reported here allow various extensions to exhaustive crossover calculations of even more complex cases and/or of other crossover functions. All this motivates a detailed presentation.

The plan of the paper is as follows: The model is presented in Sec. II and a brief qualitative discussion of the salient features concerning the possible crossover scenarios is given on the basis of the correlation function in the Gaussian approximation. Section III outlines the renormalization procedure and the Wilson β function is obtained after the renormalization of the relevant four-point vertex. In Sec. IV the effective exponent for the longitudinal susceptibility is calculated from the respective renormalized two-point vertex and its crossover behavior is studied. The limiting cases are deduced in Sec. V. A final Sec. VI presents a discussion of the results in view of recent experimental work. Important analytical procedures and calculations are given in some detail in the Appendixes A, B, C, and D.

II. MODEL

A. Hamiltonian

The critical behavior of a ferromagnet with dipolar interactions and uniaxial crystal-field anisotropy is described in momentum ($\boldsymbol{q}$) space by the effective Landau-Ginzburg-Wilson Hamiltonian[7,13,14]

$$\bar{\mathcal{H}}\{\phi\} = -\frac{1}{2}\sum_{\alpha\beta=1}^{n}\int_{\boldsymbol{q}} V_2^{\alpha\beta}(\boldsymbol{q})\,\phi_\alpha(\boldsymbol{q})\,\phi_\beta(-\boldsymbol{q}) - \frac{\lambda}{4!}\sum_{\alpha\beta\gamma\delta=1}^{n} F_{\alpha\beta\gamma\delta}\int_{\boldsymbol{q}}\int_{\boldsymbol{q}'}\int_{\boldsymbol{q}''}\phi_\alpha(\boldsymbol{q})\,\phi_\beta(\boldsymbol{q}')\,\phi_\gamma(\boldsymbol{q}'')\,\phi_\delta(-\boldsymbol{q}-\boldsymbol{q}'-\boldsymbol{q}'') \ . \tag{2}$$

The $\phi_\alpha(\boldsymbol{q})$'s are the n components of the order-parameter field which are related to the components $S_\alpha(\boldsymbol{R})$ of a spin located at a lattice point $\boldsymbol{R}$ by a Fourier transform. Below we will choose explicitly $n = d = 4 - \epsilon$ which simplifies the calculation of the one-loop integrals [see Eq. (22)]. In Eq. (2), λ is the nonlinear isotropic coupling constant, $F_{\alpha\beta\gamma\delta} = (1/3)(\delta_{\alpha\beta}\delta_{\gamma\delta} + \delta_{\alpha\gamma}\delta_{\beta\delta} + \delta_{\alpha\delta}\delta_{\beta\gamma})$, and $\int_{\boldsymbol{q}}$ stands for $\int_{-\infty}^{+\infty} \mathrm{d}^d q/(2\pi)^d$. The spin interactions are contained in the matrix

$$V_2^{\alpha\beta}(\boldsymbol{q}) = \left(r_\alpha + q^2\right)\delta_{\alpha\beta} + g\frac{q_\alpha q_\beta}{q^2} \ . \tag{3}$$

The choice of the easy axis of magnetization along the first coordinate axis specifies the r_α's as $r_1 = r$ and

$$r_j = r + m \quad \text{for} \quad 1 < j \leq n \ , \tag{4}$$

with $m > 0$ measuring the anisotropy strength, while r is proportional to the bare reduced temperature $r \sim (T - T_0)$ with the mean-field critical temperature T_0 [see Eq. (78a) for details]. Apart from a trivial shift of the critical temperature which is already included in T_0 at this stage,[7] the crucial influence of the dipolar forces is reflected in the g term in Eq. (3). The two additional characteristic lengths discussed in the Introduction are set up by the parameters m and g. One should not overlook the fact that two further terms are naturally generated when the Fourier transform of the d-dimensional dipolar interactions between moments located on a cubic lattice is considered in the relevant long-wavelength limit.[6,7] They are of the form $hq_\alpha q_\beta$ and $fq_\alpha^2\delta_{\alpha\beta}$. The first term is definitely irrelevant for the asymptotic critical behavior. The second term is of cubic symmetry and reflects the adopted underlying symmetry of the lattice. This term is known to generate a four-point vertex of cubic symmetry under the action of the RG even if such vertex is not present in the starting Hamiltonian.[14] No rigorous proof about the asymptotic irrelevance of the f term is available, although careful studies to second order of the ϵ expansion[42] or by means of the parquet-graph approximation[43] provide arguments in this direction. In any case we assume, as usual,[14] that the h and f terms do not contribute appreciably either to the asymptotic critical behavior or to the critical crossover behavior.

The free-field two-point correlation function

$$G_{\alpha\beta}^{(2)}(\boldsymbol{q},\boldsymbol{k}) = \langle\phi_\alpha(\boldsymbol{q})\phi_\beta(\boldsymbol{k})\rangle_0 = G_0^{\alpha\beta}(\boldsymbol{q})\delta(\boldsymbol{q}+\boldsymbol{k}) \tag{5}$$

in the paramagnetic phase is of paramount importance to the one-loop RG calculation of the zero-field susceptibility and, hence, of the effective susceptibility exponent γ_{eff}. In Eq. (5), $G_0^{\alpha\beta}(\boldsymbol{q})$ is the inverse of $V_2^{\alpha\beta}(\boldsymbol{q})$ and has a complicated structure when both m and g are nonzero as assumed in the present study. Namely,

$$G_0^{\alpha\beta}(\boldsymbol{q}) = \frac{1}{r_\alpha + q^2}\left[\delta_{\alpha\beta} - \frac{g}{q^2 + gQ^2}\frac{q_\alpha q_\beta}{r_\beta + q^2}\right] \ , \tag{6}$$

with

$$Q^2 = \sum_{\gamma=1}^{n}(q_\gamma)^2/(r_\gamma + q^2) \ ,$$

where the r_α's are defined in Eq. (4). As explained in Ref. 7, the expression (6) for the correlation function is nonanalytic in the limit $\boldsymbol{q} \to 0$ in that its limiting value depends upon the direction from which the wave vector approaches zero. At $\boldsymbol{q} = 0$,

$$G_0^{\alpha\beta}(0) = \frac{1}{r_\alpha + g\,N_{\alpha\alpha}}\,\delta_{\alpha\beta} \ . \tag{7}$$

The quantity $N_{\alpha\alpha}$ has the simple interpretation of being

the respective diagonal component of the demagnetizing tensor for the considered sample only in the case when the latter is an ellipsoid whose principal axes coincide with the anisotropy axes. In the general case $N_{\alpha\alpha}$ is given by complex lattice sums.

B. Gaussian approximation

The correlation function of Eq. (6) contains all important details concerning the Gaussian critical behavior, i.e., the criticality of the noninteracting ($\lambda = 0$) fluctuation model. It is instructive to present the analysis of the free-field case.[1,12,14] Among other things, this serves to establish salient qualitative features of the possible crossover scenarios and to naturally introduce relevant terminology and relations.

Let us now concentrate on the Gaussian correlations for three-component systems ($n = 3$). By dimensional considerations, one has

$$G_0^{\alpha\beta}(\boldsymbol{q}; r, m, g) = \xi^2 \cdot G_0^{\alpha\beta}\left(q^2\xi^2; 1, \frac{m}{r}, \frac{g}{r}\right) , \qquad (8)$$

where the correlation length $\xi = r^{-1/2} \sim (T - T_0)^{-1/2}$ diverges for $T \to T_0$ with the mean-field critical exponent $\nu = 1/2$. For $r \gg g$, one finds different correlations along and perpendicular to the easy axis as seen in the expressions for the two-point correlation functions, respectively:

$$G_{11}^{(2)}(\boldsymbol{q}, \boldsymbol{k}) = \frac{\xi^2}{1 + q^2\xi^2}\, \delta(\boldsymbol{q} + \boldsymbol{k}) , \qquad (9)$$

$$G_{jj}^{(2)}(\boldsymbol{q}, \boldsymbol{k}) = \frac{\xi^2}{1 + \frac{m}{r} + q^2\xi^2}\, \delta(\boldsymbol{q} + \boldsymbol{k}) . \qquad (10)$$

The index j with $1 < j \leq n$ stands for the different perpendicular directions. An isotropic two-point correlation function for any combination of components derives from Eqs. (9) and (10) if, additionally, $r \gg m$ so that for sufficiently high temperatures both uniaxial and dipolar interactions are suppressed in the correlation function

$$G_{\alpha\beta}^{(2)}(\boldsymbol{q}, \boldsymbol{k}) = \frac{\xi^2}{1 + q^2\xi^2}\, \delta_{\alpha\beta}\, \delta(\boldsymbol{q} + \boldsymbol{k}) \qquad (11)$$

and one expects to detect critical behavior typical for the Heisenberg model.

As $r \to 0$ ($T \to T_0$), one has to specify the relative magnitude of the parameters m and g which indicate the strength of the anisotropy and the dipolar interaction respectively. Considering the extremes for the ratio m/g, there emerge two generic crossover scenarios as the reduced temperature variable decreases to zero. The situation is depicted in Fig. 1.

For $m \gg g$, one has to consider next the temperature range specified by the inequalities $m \gg r \gg g$ and Eq. (10) indicates that the perpendicular correlation function $G_{jj}^{(2)}$ vanishes in this limit. As only spin components along the easy axis are then correlated, this regime is characterized as Ising critical behavior. Therefore, a

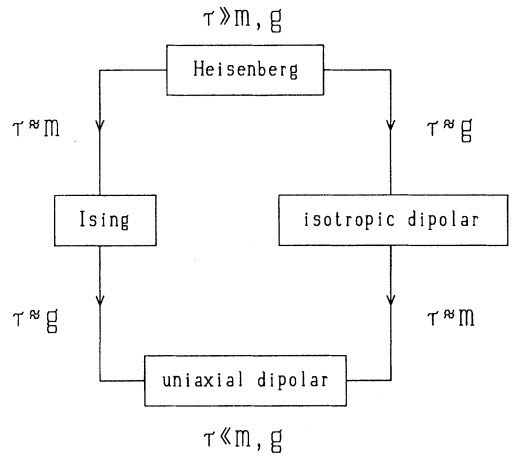

FIG. 1. Qualitative crossover scenarios as seen in the Gaussian analysis of the problem. Going beyond the zeroth order of the perturbation theory, the mean-field temperature scale $r \sim (T - T_0)$ has to be replaced by the renormalized temperature scale $\tau \sim (T - T_c)$.

crossover from Heisenberg to Ising critical behavior is expected to occur for $r \approx m$. In the Ising critical regime ($m \gg r \gg g$) one obtains from Eq. (6)

$$G_{11}^{(2)}(\boldsymbol{q}, \boldsymbol{k}) = \frac{\xi^2}{1 + \frac{g}{r}\frac{(q_1)^2}{q^2} + q^2\xi^2}\, \delta(\boldsymbol{q} + \boldsymbol{k}) , \qquad (12)$$

which is the well-known correlation function for the dipolar Ising system. If the temperature is further reduced, so that now both $m, g \gg r$, Eq. (12) implies that the longitudinal correlation function vanishes for wave vectors $\boldsymbol{q}$ parallel to the easy axis. Nonzero longitudinal correlations persist only for wave vectors which are transverse to the easy axis ($q_1 = 0$). Such a growth of the transverse-$\boldsymbol{q}$ contribution to the correlation function is typical for dipolar systems. The regime $m, g \gg r$ is then denoted as *uniaxial dipolar* critical behavior. It is exactly in this case that one expects mean-field asymptotic behavior with logarithmic corrections. Obviously, a further crossover should have occurred in between, namely, the crossover from Ising to uniaxial dipolar behavior at $r \approx g$.

For $m \ll g$, the system starts out with the Heisenberg regime for $r \gg m, g$, as commented above [Eq. (11)], and then crosses over at $r \approx g$ to an isotropic dipolar behavior as can be recognized in the corresponding form of the two-point correlation function:

$$G_{\alpha\beta}^{(2)}(\boldsymbol{q}, \boldsymbol{k}) = \frac{\xi^2}{1 + q^2\xi^2}\left[\delta_{\alpha\beta} - \frac{q_\alpha q_\beta}{q^2}\right] \delta(\boldsymbol{q} + \boldsymbol{k}) . \qquad (13)$$

Upon further lowering of the temperature, one reaches once again the asymptotic uniaxial dipolar behavior (cf. Fig. 1).

As already stated in the Introduction, it is our intention to characterize quantitatively the crossover behavior in the system described by the model (2) by calculating the temperature-dependent effective critical exponent for

the susceptibility. The tensor of the inverse susceptibility $\chi^{-1}_{\alpha\beta}$ is defined with respect to the internal magnetic field. In the paramagnetic phase it is given by

$$\chi^{-1}_{\alpha\beta} = \frac{1}{g}\left[G^{(2)}_{\alpha\beta}(\boldsymbol{k}=0)\right]^{-1} - N_{\alpha\alpha}\delta_{\alpha\beta} \ , \tag{14}$$

with the second term being the usual demagnetization correction. In the Gaussian regime, according to Eqs. (5) and (7),

$$\chi^{-1}_{11} = r/g \ , \tag{15}$$

$$\chi^{-1}_{jj} = (r+m)/g \ . \tag{16}$$

At $r=0$ ($T=T_0$), it is only the component of the susceptibility parallel to the easy axis that diverges. This statement holds beyond the Gaussian regime.[14] Introducing the reduced temperature scale referred to the true critical temperature T_c by $\tau \sim (T-T_c)$, the singularity of χ_{11} is characterized by the critical exponent γ according to the usual definition $\chi_{11} \sim |\tau|^{-\gamma}$. The behavior of the other components of the susceptibility tensor will not be discussed here; the reader is referred to Refs. 10, 44–47 for further discussion of this issue.

The results of the Gaussian analysis of the correlations in the critical region can now be applied to obtain qualitative predictions about how the expected crossover schemes (Fig. 1) would reflect upon the value of the effective critical exponent $\gamma_{\rm eff}$ defined in Eq. (1). In the range $\tau \gg m, g$ and regardless of the ratio m/g, one expects that $\gamma_{\rm eff} = \gamma_H$. For $m \gg g$, the crossover as seen in the value of $\gamma_{\rm eff}$ should proceed as $\gamma_H \to \gamma_I \to \gamma_{\rm UD}$, while for $m \ll g$ the sequence should be $\gamma_H \to \gamma_{\rm ID} \to \gamma_{\rm UD}$. Here, the subscripts H, I, ID, and UD stand for "Heisenberg," "Ising," "isotropic dipolar," and "uniaxial dipolar," respectively. If the parameters m and g are of the same order of magnitude, no two-stage crossover structure is to be expected as the problem is then an effectively single-parameter one. There is then a single crossover $\gamma_H \to \gamma_{\rm UD}$ which corresponds to the crossover from Heisenberg to uniaxial dipolar behavior. Asymptotically, $\gamma_{\rm UD}$ takes on the mean-field value of unity but this proceeds slowly on the τ scale because of the logarithmic corrections. In fact, all qualitative predictions for the special case $m=g$ have been corroborated quantitatively by a recent explicit one-loop calculation of $\gamma_{\rm eff}$.[38]

III. THE RENORMALIZATION FLOW IN PARAMETER SPACE

Renormalized-field theory[48,49] is applied to determine the parameter flow, the fixed points, and the effective critical exponent for the longitudinal zero-field susceptibility of the system described by (2) to the order of one loop. The propagator is the one defined by Eq. (6). Two vertex functions have to be determined and renormalized, the four-point vertex $\Gamma^{(4)}_{1111}(\boldsymbol{k}_1,\boldsymbol{k}_2,\boldsymbol{k}_3,\boldsymbol{k}_4)$ and the two-point vertex $\Gamma^{(2)}_{11}(\boldsymbol{k}_1,\boldsymbol{k}_2)$. When duly renormalized and taken at zero momenta, the former yields the RG flow equation for the ϕ^4-coupling constant, while the latter gives the inverse longitudinal susceptibility itself. Combining the information from both gives finally $\gamma_{\rm eff}$.

The emerging one-loop integrals are calculated with the help of dimensional regularization and ϵ expansion with $\epsilon = 4-d$ and d indicating the dimensionality of space. An infinite cutoff is used and, hence, renormalization has to be performed. As in the simpler models studied earlier,[28,31] no renormalization of m and g is necessary. The N-point vertex functions $\Gamma^{(N)}$, the temperature variable r, and the ϕ^4-coupling constant λ are renormalized multiplicatively with the renormalizing factors Z_ϕ, Z_{ϕ^2}, and Z_u which are defined as usual:[48]

$$\Gamma^{(N)}_R = Z^{N/2}_\phi \Gamma^{(N)} \ , \tag{17a}$$

$$\bar{r} = Z_{\phi^2}\tau \ , \tag{17b}$$

$$\lambda = Z_u \kappa^\epsilon S_d^{-1} u \ . \tag{17c}$$

In Eq. (17b), $\bar{r}$ is the shifted reduced temperature,

$$\bar{r} = r - gN_{11} + \Gamma^{(2)}_{11}(\boldsymbol{k}=0; r=0, m, g) \ , \tag{18}$$

while $\Gamma^{(N)}_R$, τ, and u are the respective renormalized quantities. The geometric factor is the usual $S_d^{-1} = 2^{d-1}\pi^{d/2}\Gamma(d/2)$ with $\Gamma(z)$ the gamma function, $\epsilon = 4-d$, and κ is an arbitrary momentum. In the critical region and within the ϵ-expansion scheme, u is of the first order in ϵ and the renormalizing multiplicative factors are of the form

$$Z_\phi = 1 + O(u^2) \ , \tag{19a}$$

$$Z_{\phi^2} = 1 + c_1 u + O(u^2) \ , \tag{19b}$$

$$Z_u = 1 + a_1 u + O(u^2) \ . \tag{19c}$$

The first equation simply means that the anomalous dimensionality of the order-parameter (OP) field does not show up in the one-loop calculation. It remains then to determine the renormalizing factors Z_{ϕ^2} and Z_u or, which is the same, c_1 and a_1. In principle, these constants are determined from the one-loop contributions to the two- and four-point vertices, respectively. The most convenient way of doing this is the method of minimal subtraction invented by 't Hooft and Veltmann.[50] Within this approach only the poles of the vertex functions which are of the form $1/\epsilon$ and lead to divergencies in the limit $d \to 4$ are considered. For the application to systems with crossover behavior, Amit and Goldschmidt[28] developed the method of generalized minimal subtraction (GMS). To understand their ideas, the flow of the parameters under a transformation $\boldsymbol{k}_i \to \rho \boldsymbol{k}_i$ of the length scale has to be considered. It follows from naive dimensional analysis that

$$m(\rho) = \frac{m}{\rho^2} \qquad \text{and} \qquad g(\rho) = \frac{g}{\rho^2} \ , \tag{20}$$

and the critical region is found in the long-wavelength limit $\rho \to 0$. The critical region therefore corresponds to the region of infinite anisotropic and dipolar coupling constants. Consequently, in addition to the poles appearing in the limit $\epsilon \to 0$, the divergences showing up for $m \to \infty$ and $g \to \infty$ have also to be subtracted within the GMS scheme. A prerequisite for the implementation of the GMS method is the temperature shift given by Eq. (18) whose physical meaning is the fixing of true criticality at $\bar{r} = 0$ or, as follows from Eq. (17b), at $\tau = 0$.[28]

It will be seen (Sec. IV) that it is not necessary to determine c_1 explicitly in order to find γ_{eff} to one-loop order. This is a considerable simplification because of the rather complicated nature of the perturbation integrals which have to be considered. This aspect of the calculation of γ_{eff} has remained unnoticed in the simpler limiting cases considered earlier within the GMS scheme (dominant anisotropy in $\bar{n} < n$ components of the OP,[28] isotropic dipolar ferromagnet,[31] and Ising dipolar ferromagnet[34]). It is therefore an improvement over previous treatments as well.

It is now clear that it remains to determine the renormalizing factor Z_u (i.e., the constant a_1) from the one-loop contribution to $\Gamma^{(4)}_{1111}(\boldsymbol{k}_i = 0)$:

$$\Gamma^{(4)}_{1111}\left(0; \frac{r}{\kappa^2}, \frac{m}{\kappa^2}, \frac{g}{\kappa^2}, \frac{\lambda}{\kappa^\epsilon}\right) = \frac{\lambda}{\kappa^\epsilon} - \frac{3}{2}\left(\frac{\lambda}{\kappa^\epsilon}\right)^2 \int_q \Bigg[G_0^{11}(\boldsymbol{q})\, G_0^{11}(\boldsymbol{q}) + \frac{2(n-1)}{3} G_0^{1j}(\boldsymbol{q})\, G_0^{1j}(\boldsymbol{q}) + \frac{n-1}{9} G_0^{jj}(\boldsymbol{q})\, G_0^{jj}(\boldsymbol{q}) + \frac{(n-1)(n-2)}{9} G_0^{jj'}(\boldsymbol{q})\, G_0^{jj'}(\boldsymbol{q}) \Bigg] . \tag{21}$$

In deriving Eq. (21), the obvious symmetry $G_0^{\alpha\beta} = G_0^{\beta\alpha}$ has been used. The $n-1$ directions perpendicular to the easy axis are indicated by j, j' with $j \neq j'$. The integration can be further simplified, with $n = d = 4 - \epsilon$, by noting that

$$Q^2 = \sum_{\gamma=1}^{d} \frac{(q_\gamma)^2}{r_\gamma + q^2} = \frac{(q_1)^2}{r + q^2} + \frac{q^2 - (q_1)^2}{r + m + q^2} , \tag{22}$$

which means that it is only the modulus $q = |\boldsymbol{q}|$ and one angle $\theta = \arccos(q_1/q)$ which appear explicitly in the denominator of the propagator [Eq. (6)]. Carrying out in Eq. (21) the angular integration in the plane perpendicular to the easy (q_1) axis, one obtains

$$\Gamma^{(4)}_{1111}\left(0; \frac{r}{\kappa^2}, \frac{m}{\kappa^2}, \frac{g}{\kappa^2}, \frac{\lambda}{\kappa^\epsilon}\right) = \frac{\lambda}{\kappa^\epsilon} - \frac{3}{2}\left(\frac{\lambda}{\kappa^\epsilon}\right)^2 \left[I_0 - I_1 + I_2 + 2I_3 + \frac{1}{3}\bar{I}_0 - \frac{1}{3}I_4 + \frac{5}{3}I_5 \right] , \tag{23}$$

where the integrals $I_i(r/\kappa^2, m/\kappa^2, g/\kappa^2)$ are defined in Appendix A. It is not necessary to calculate exactly the I_i's within the framework of the GMS scheme. All one needs is to determine those contributions to the integrals which diverge for $\epsilon \to 0$, $m \to \infty$, and/or $g \to \infty$. In these limits, the divergences are simple poles in ϵ, while they are logarithmic in m, g, and $(m+g)$. Their calculation is presented in sufficient detail in Appendix A. The result for the divergent contributions to $\Gamma^{(4)}_{1111}$ is

$$\Gamma^{(4)\text{div}}_{1111}\left(0; \frac{r}{\kappa^2}, \frac{m}{\kappa^2}, \frac{g}{\kappa^2}, \frac{\lambda}{\kappa^\epsilon}\right) = \frac{\lambda}{\kappa^\epsilon} - \frac{3S_d}{4}\left(\frac{\lambda}{\kappa^\epsilon}\right)^2 \left[\frac{8}{3}\frac{1}{\epsilon} - \ln\left(\frac{r+g}{\kappa^2}\right) - \frac{17}{18}\ln\left(\frac{r+m}{\kappa^2}\right) + \frac{11}{18}\ln\left(\frac{r+m+g}{\kappa^2}\right) \right] . \tag{24}$$

Having in mind the definitions of u and Z_u [Eqs. (17c) and (19c)], one obtains the following expression for the constant a_1:

$$a_1\left(\frac{\sqrt{m}}{\kappa}, \frac{\sqrt{g}}{\kappa}\right) = \frac{2}{\epsilon} - \frac{3}{2\sigma}\ln\left[1 + \left(\frac{g}{\kappa^2}\right)^{\sigma/2}\right] - \frac{17}{12\sigma}\ln\left[1 + \left(\frac{m}{\kappa^2}\right)^{\sigma/2}\right] + \frac{11}{12\sigma}\ln\left[1 + \left(\frac{m+g}{\kappa^2}\right)^{\sigma/2}\right] . \tag{25}$$

This choice of a_1 guarantees that the four-point function (23) is finite for $\epsilon \to 0$ and in the limits $m \to \infty$ and $g \to \infty$ and, hence, $\Gamma^{(4)}_{1111}$ is renormalized in the sense of the GMS scheme. This holds for arbitrary values of σ. As already mentioned in Ref. 34, in order to obtain the logarithmic corrections in the uniaxial-dipolar limit, one has to choose $\sigma = 1$. Now the Wilson β function is calculated as[48]

$$\beta\left(u, \frac{\sqrt{m}}{\kappa}, \frac{\sqrt{g}}{\kappa}\right) = \kappa \left.\frac{\partial u}{\partial \kappa}\right|_{\lambda, m, g} , \tag{26}$$

with the result

$$\beta\left(u,\frac{\sqrt{m}}{\kappa},\frac{\sqrt{g}}{\kappa}\right)=-\epsilon u+u^2\left[\frac{3}{2}\frac{1}{1+\frac{\sqrt{g}}{\kappa}}+\frac{17}{12}\frac{1}{1+\frac{\sqrt{m}}{\kappa}}-\frac{11}{12}\frac{1}{1+\frac{\sqrt{m+g}}{\kappa}}\right]+O\left(\epsilon u^2,u^3\right)\ . \tag{27}$$

The flow of the renormalized coupling constant u under a transformation $\boldsymbol{k}\to\rho\boldsymbol{k}$ of all lengths is described by the flow equation[28]

$$\rho\frac{\mathrm{d}u(\rho)}{\mathrm{d}\rho}=\beta\left(u(\rho),\frac{\sqrt{m}}{\kappa\rho},\frac{\sqrt{g}}{\kappa\rho}\right)\ , \tag{28}$$

whose solution at $\epsilon=1$ is

$$u^{-1}(\rho)=\frac{\rho}{u}+\frac{3}{2}\frac{\kappa\rho}{\sqrt{g}}\ln\left[\frac{1+\frac{\sqrt{g}}{\kappa\rho}}{1+\frac{\sqrt{g}}{\kappa}}\right]+\frac{17}{12}\frac{\kappa\rho}{\sqrt{m}}\ln\left[\frac{1+\frac{\sqrt{m}}{\kappa\rho}}{1+\frac{\sqrt{m}}{\kappa}}\right]-\frac{11}{12}\frac{\kappa\rho}{\sqrt{m+g}}\ln\left[\frac{1+\frac{\sqrt{m+g}}{\kappa\rho}}{1+\frac{\sqrt{m+g}}{\kappa}}\right]\ , \tag{29}$$

where $u(\rho=1)=u$.

The character of the RG flow of the renormalized coupling constant $u(\rho)$ reflects the structure of the critical region and provides, even before the calculation of γ_{eff}, for abundant information about the different crossover regimes discussed qualitatively in Sec. II (cf Fig. 1). The backbone of the structure consists of the four nontrivial fixed points which are defined as the zeros of the Wilson β function. These are (i) Heisenberg, $u_H^*=\epsilon/2$ for $\kappa\rho\gg m^{1/2},g^{1/2}$; (ii) Ising, $u_I^*=2\epsilon/3$ for $m^{1/2}\gg\kappa\rho\gg g^{1/2}$; (iii) isotropic dipolar, $u_{\mathrm{ID}}^*=12\epsilon/17$ for $g^{1/2}\gg\kappa\rho\gg m^{1/2}$; and (iv) uniaxial dipolar with $u_{\mathrm{UD}}^*\to\infty$ ($u_{\mathrm{UD}}^*\sim 1/\rho\ln\rho$ with $\rho\to 0$ for $m^{1/2},g^{1/2}\gg\kappa\rho$). When both m and g are nonzero, the renormalization flow goes ultimately to u_{UD}^*, thus establishing the asymptotic domination of the joint influence of dipolar interactions and uniaxial anisotropy. The critical region for the crossover problem is characterized by the condition

$$\rho\ll\min\left[1,\frac{u}{|u-u_H^*|}\right]\ , \tag{30}$$

which guarantees universality of the flow in the sense that there $u(\rho)$ is independent of the initial value u and the crossover scaling functions are universal.[12] In fact, $\rho\ll 1$ corresponds to the physical expectation that only large wavelengths are important in the vicinity of a phase transition, while $\rho\ll u/|u-u_H^*|$ corresponds basically to the condition that the system in consideration be critical even if anisotropy and dipolar interactions are switched off *and* the system be initially close to Heisenberg criticality. Now we have to recall the fact that u is related to the coupling constant λ of the initial Hamiltonian as well as to the arbitrary momentum κ [Eq. (17c)]. Therefore it is not possible to estimate the value of u for a given bare system and we have to consider u as a free parameter of the renormalized-field theory. Consequently, neither the width of the critical region nor the precise trajectory can be exactly predicted. The choice of $u=u_H^*$ provides for an as large as possible critical region while on the other hand for $u=0$ the critical region vanishes, corresponding to the unstable Gaussian fixed point. In view of the uncertainties with respect to the choice of u, it might be rewarding to pursue, within the more general and quantitative context of the results in this paper, the semiempirical procedure of fixing the initial value of $u(\rho)$ by fitting to a relevant set of experimental data.[51]

Since the coupling constant $u(\rho)$, diverges in the asymptotic limit $\rho\to 0$, it is convenient for graphical representations to use the effective renormalized coupling constant[34]

$$w(\rho)=\frac{u(\rho)}{1+\frac{\sqrt{g}}{\kappa\rho}}\ , \tag{31}$$

which is finite in the entire parameter region. The asymptotic values of $w(\rho)$ are $w(\rho)\approx u(\rho)$ for $\rho\gg g^{1/2}/\kappa$ and $w(\rho)\sim(\gamma_{\mathrm{eff}}-1)$ for $\rho\ll g^{1/2}/\kappa$. The second limit can be identified by considering our result for γ_{eff} in the respective limit [Eq. (76)]. In Fig. 2 the effective coupling constant $w(\rho)$ as given by Eqs. (31) and (29) is displayed for $g=10^{-12}$ and different values of m (whereby $\kappa=1$ and $u=u_H^*$). The curve with $m=10^{-2}$ exhibits a well-expressed crossover for $\rho^2\approx m$ to short-range Ising behavior dominated by u_I^*. For $\rho^2\approx g$, $w(\rho)$ goes over to zero, signaling a mean-field critical behavior with logarithmic corrections as verified below. For smaller values of the anisotropy parameter m the plateau of effective Ising behavior becomes smaller and finally disappears. The influence of the initial value u of the coupling constant on the flow of $w(\rho)$ is illustrated in Fig. 3. The curve with $u=u_H^*$ is the same as in Fig. 2. One notes that although both the width of the critical region and the character of the corresponding trajectories are sensitive to the initial value of $u(\rho)$, the trajectories are totally independent of it inside the critical region as given by $\rho\ll u/|u-u_H^*|$. The influence of the parameters u and

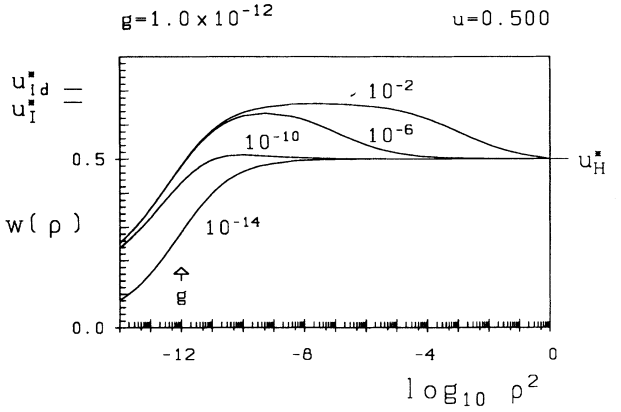

FIG. 2. The flow of the effective coupling constant $w(\rho)=u(\rho)/(1+\sqrt{g}/\kappa\rho)$ for $g=10^{-12}$, $u=u_H^*=1/2$, and different values of m.

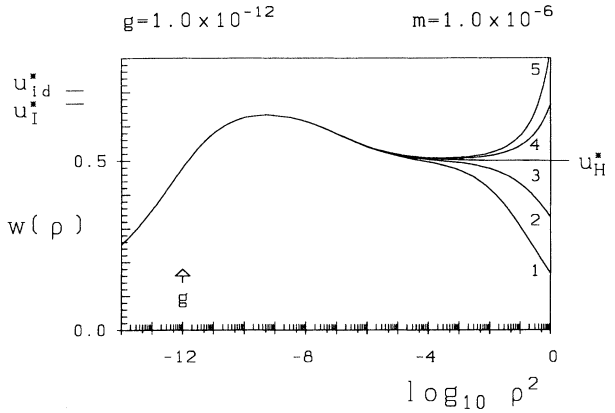

FIG. 3. The flow of the effective coupling constant $w(\rho) = u(\rho)/(1 + \sqrt{g}/\kappa\rho)$ for $g = 10^{-12}$ and $m = 10^{-6}$. The curves have been calculated for different values of the coupling constant $u = k/6$ with k indicated next to each curve.

κ on the effective exponent γ_{eff} will be discussed in Sec. IV C.

IV. EFFECTIVE EXPONENT FOR THE ZERO-FIELD EASY-AXIS SUSCEPTIBILITY

The temperature dependence of the inverse easy-axis susceptibility χ_{11}^{-1} is described by the effective exponent γ_{eff} defined in Eq. (1). The tensor $\chi_{\alpha\beta}^{-1}$ is to be calculated from the two-point vertex function taken at zero momentum according to

$$\chi_{\alpha\beta}^{-1}(r, m, g, \lambda) = \frac{1}{g}\,\Gamma_{\alpha\beta}^{(2)}(\boldsymbol{k} = 0) - N_{\alpha\alpha}\delta_{\alpha\beta}\ , \qquad (32)$$

as follows from Eq. (14) and Ref. 48. To the order of one loop, the component of $\Gamma_{\alpha\beta}^{(2)}$ along the easy axis is given by

$$\Gamma_{11}^{(2)}(\boldsymbol{k} = 0; r, m, g, \lambda) = r + gN_{11} + \lambda\Psi(r, m, g) \qquad (33)$$

and the demagnetization factor N_{11} cancels in Eq. (32). The function $\Psi(r, m, g)$ contains the contributions from the perturbation integrals.

A. General considerations

The derivation of γ_{eff} presented here is in fact very general and holds for any system with crossover behavior provided that the parameters (here m and g) which bring about the crossover need not be additionally renormalized. Now we proceed to derive in some detail an intermediate expression for γ_{eff} [Eq. (53)] which, beside its generality, is important for further analytical treatment, i.e. for the derivation of the final result given in Eq. (62).

Shifting to the true reduced temperature $\bar{r}$ according to Eq. (18), one rewrites the two-point vertex to the order of one loop as

$$\Gamma_{11}^{(2)}(0; \bar{r}, m, g, \lambda) = \bar{r} + gN_{11} + \lambda\Sigma(\bar{r}, m, g)\ , \qquad (34)$$

where

$$\Sigma(\bar{r}, m, g) = \Psi(\bar{r}, m, g) - \Psi(0, m, g)\ . \qquad (35)$$

The renormalized temperature τ and the coupling constant u were already defined in Eqs. (17b) and (17c) in which at the same time the renormalizing factors Z_{ϕ^2} and Z_u were introduced. These are represented as series in u [Eqs. (19b),(19c)] with

$$c_1 = c_1\left(\frac{\sqrt{m}}{\kappa}, \frac{\sqrt{g}}{\kappa}\right), \quad a_1 = a_1\left(\frac{\sqrt{m}}{\kappa}, \frac{\sqrt{g}}{\kappa}\right)\ . \qquad (36)$$

By dimensionality, one has

$$\Gamma_{\alpha\beta}^{(2)}(\boldsymbol{k}; \bar{r}, m, g, \lambda) = \kappa^2\,\Gamma^{(2)}\left(\frac{\boldsymbol{k}}{\kappa}; \frac{\bar{r}}{\kappa^2}, \frac{m}{\kappa^2}, \frac{g}{\kappa^2}, \frac{\lambda}{\kappa^\epsilon}\right) \qquad (37)$$

and

$$\frac{\kappa^\epsilon}{\kappa^2}\Sigma(\bar{r}, m, g) = \Sigma\left(\frac{\bar{r}}{\kappa^2}, \frac{m}{\kappa^2}, \frac{g}{\kappa^2}\right)\ . \qquad (38)$$

The dimensionless renormalized vertex to first order in u is therefore given by

$$\Gamma_{11,R}^{(2)}\left(0; \frac{\tau}{\kappa^2}, \frac{m}{\kappa^2}, \frac{g}{\kappa^2}, u\right) = \frac{\tau + gN_{11}}{\kappa^2} + \left[c_1\left(\frac{\sqrt{m}}{\kappa}, \frac{\sqrt{g}}{\kappa}\right)\frac{\tau}{\kappa^2} + \frac{1}{S_d}\Sigma\left(\frac{\tau}{\kappa^2}, \frac{m}{\kappa^2}, \frac{g}{\kappa^2}\right)\right]u\ . \qquad (39)$$

The renormalized vertex transforms as

$$\Gamma_{11,R}^{(2)}\left(0; \frac{\tau}{\kappa^2}, \frac{m}{\kappa^2}, \frac{g}{\kappa^2}, u\right) = \rho^2\,\Gamma_{11,R}^{(2)}\left(0; \frac{\tau(\rho)}{\kappa^2}, \frac{m(\rho)}{\kappa^2}, \frac{g(\rho)}{\kappa^2}, u(\rho)\right) \qquad (40)$$

under an arbitrary change of the length scale with the factor ρ: $\boldsymbol{k}_i \to \rho\boldsymbol{k}_i$. As to the "flowing" arguments in the right-hand side of the last equation, (i) there is no need to additionally renormalize m (Ref. 28) and g (Refs. 31, 34) which means that their flow follows from naive dimensional analysis as given in Eq. (20); (ii) the coupling constant $u(\rho)$ satisfies the flow equation (28) which was already solved with the result given in Eq. (29); (iii) the RG flow of $\tau(\rho)$ has to be determined as usual from[28,48]

$$\tau(\rho) = \frac{\tau}{\rho^2}\exp\left[\int_1^\rho \frac{dx}{x}\gamma_{\phi^2}\left(u(x), \frac{\sqrt{m}}{x}, \frac{\sqrt{g}}{x}\right)\right]\ , \qquad (41)$$

where the Wilson γ_{ϕ^2} function is defined by

$$\gamma_{\phi^2} = -\kappa\left.\frac{\partial \ln Z_{\phi^2}}{\partial\kappa}\right|_{m,g,\lambda}\ . \qquad (42)$$

With Eqs. (17c) and (19b) and to first order in u,

$$\gamma_{\phi^2} = \epsilon u\, c_1\left(\frac{\sqrt{m}}{\kappa}, \frac{\sqrt{g}}{\kappa}\right) - u\kappa \left.\frac{\partial c_1}{\partial \kappa}\right|_{m,g} . \tag{43}$$

The $1/\epsilon$ pole of c_1 is the same as in the case of short-range spin systems,[28,31] i.e.,

$$c_1\left(\frac{\sqrt{m}}{\kappa}, \frac{\sqrt{g}}{\kappa}\right) = \frac{n+2}{6\epsilon} + O\left(\epsilon^0\right) . \tag{44}$$

Therefore, neglecting terms of order ϵu, one has

$$\gamma_{\phi^2} = \frac{n+2}{6} u - u\kappa \left.\frac{\partial c_1}{\partial \kappa}\right|_{m,g} . \tag{45}$$

Imposing the matching condition $\tau(\rho) = \kappa^2$, one obtains, from Eq. (40) and Eq. (20),

$$\Gamma^{(2)}_{11,R}\left(0; \frac{\tau}{\kappa^2}, \frac{m}{\kappa^2}, \frac{g}{\kappa^2}, u\right)$$

$$= \rho^2\, \Gamma^{(2)}_{11,R}\left(0; 1, \frac{m}{\kappa^2\rho^2}, \frac{g}{\kappa^2\rho^2}, u(\rho)\right) \tag{46}$$

and, from Eq. (41),

$$\rho^2 = \frac{\tau}{\kappa^2} \exp\left[\int_1^\rho \frac{dx}{x} \gamma_{\phi^2}\left(u(x), \frac{\sqrt{m}}{x}, \frac{\sqrt{g}}{x}\right)\right] . \tag{47}$$

Since γ_{ϕ^2} is of order u, the approximation $\rho^2 \approx \tau/\kappa^2$ holds up to the order u^0. Now one rewrites the expression (32) for the inverse easy-axis susceptibility in terms of the renormalized dimensionless vertex function $\Gamma^{(2)}_{11,R}$ as

$$\chi^{-1}_{11}(\tau, m, g, u) = \frac{\kappa^2}{g}\, \Gamma^{(2)}_{11,R}\left(0; \frac{\tau}{\kappa^2}, \frac{m}{\kappa^2}, \frac{g}{\kappa^2}, u\right) - N_{11} \tag{48}$$

and uses Eq. (46) and the definition (1) to derive the expression

$$\gamma_{\text{eff}} = \frac{\mathrm{d}\ln\rho^2}{\mathrm{d}\ln\tau} + \frac{\mathrm{d}}{\mathrm{d}\ln\tau} \times \ln\left[\Gamma^{(2)}_{11,R}\left(0; 1, \frac{m}{\kappa^2\rho^2}, \frac{g}{\kappa^2\rho^2}, u(\rho)\right) - \frac{gN_{11}}{\kappa^2\rho^2}\right] . \tag{49}$$

In view of Eq. (47), the first term in the last equation is

$$\frac{\mathrm{d}\ln\rho^2}{\mathrm{d}\ln\tau} = 1 + \frac{1}{2}\gamma_{\phi^2}\left(u(\rho), \frac{\sqrt{m}}{\kappa\rho}, \frac{\sqrt{g}}{\kappa\rho}\right) , \tag{50}$$

where $\tau^{1/2}/\kappa$ was substituted for ρ at the upper limit of integration in Eq. (47). This is justifiable to one-loop order.[28] For the second term in Eq. (49), one uses Eq. (39) and obtains up to first order in u and ϵ

$$\frac{\mathrm{d}}{\mathrm{d}\ln\tau} \ln\left[\Gamma^{(2)}_{11,R}\left(0; 1, \frac{m}{\kappa^2\rho^2}, \frac{g}{\kappa^2\rho^2}, u(\rho)\right) - \frac{gN_{11}}{\kappa^2\rho^2}\right]$$

$$= \rho^2 u(\rho)\, \frac{\partial}{\partial\rho^2} c_1\left(\frac{\sqrt{m}}{\kappa\rho}, \frac{\sqrt{g}}{\kappa\rho}\right) + \frac{\rho^2 u(\rho)}{S_d}\, \frac{\partial}{\partial\rho^2} \Sigma\left(1, \frac{m}{\kappa^2\rho^2}, \frac{g}{\kappa^2\rho^2}\right) . \tag{51}$$

The contribution containing the derivative $\partial u(\rho)/\partial\rho^2$ is neglected, since it is of second order in ϵ. Now note that

$$\frac{\partial}{\partial\rho^2} c_1\left(\frac{\sqrt{m}}{\kappa\rho}, \frac{\sqrt{g}}{\kappa\rho}\right) = \frac{\kappa}{2\rho^2}\frac{\partial}{\partial\kappa} c_1\left(\frac{\sqrt{m}}{\kappa\rho}, \frac{\sqrt{g}}{\kappa\rho}\right) , \tag{52}$$

so that according to Eqs. (45), (50), and (51) all terms containing $\partial c_1/\partial\kappa$ in Eq. (49) for γ_{eff} cancel out exactly to the order considered. As the second term in Eq. (51) is also needed to $O(u^1)$ only, ρ is set equal to $\tau^{1/2}/\kappa$ with the result

$$\gamma_{\text{eff}} = 1 + \left[\frac{n+2}{12} + S\left(\frac{m}{\tau}, \frac{g}{\tau}\right)\right] u\left(\frac{\sqrt{\tau}}{\kappa}\right) , \tag{53}$$

where

$$S\left(\frac{m}{\tau}, \frac{g}{\tau}\right) = \frac{\tau}{S_d}\, \frac{\partial\Sigma\left(1, \frac{m}{\tau}, \frac{g}{\tau}\right)}{\partial\tau} . \tag{54}$$

The result for γ_{eff} as given by Eq. (53) simplifies the further calculations considerably, because it is now evident that, as stated in Sec. III, the renormalizing factor Z_{ϕ^2} or, which is the same to this order, the coefficient c_1 need not to be calculated explicitly. Obviously, the same holds for the simpler cases of crossover calculations of γ_{eff} studied earlier. Hence, Eq. (53) represents both an extension and an improvement over existing one-loop calculations of the effective critical exponent of the zero-field longitudinal susceptibility. The problem can now be seen to lie with the determination of the renormalizing factor Z_u *and* the integrals hidden in Σ [Eqs. (34) and (35)]. As Z_u and $u(\rho)$ were already calculated in the previous section, it remains to deal with the said integrals.

B. Calculation of the effective exponent

To this end, one has to step back and recall that to the order of one loop the two-point vertex $\Gamma^{(2)}_{11}$ is given by

$$\Gamma^{(2)}_{11}(\boldsymbol{k} = 0; r, m, g, \lambda) = r + gN_{11} + \frac{\lambda}{2} \sum_{\alpha,\beta=1}^{n} \int_{\boldsymbol{q}} F_{11\alpha\beta} \times G_0^{\alpha\beta}(\boldsymbol{q}, r, m, g) . \tag{55}$$

Shifting the temperature scale to $\bar{r}$ according to Eq. (18) and carrying out the summation, one obtains

$$\Gamma_{11}^{(2)}(0;\bar{r},m,g,\lambda) = \bar{r} + gN_{11} + \frac{1}{2}\lambda\int_{\boldsymbol{q}}\left[G_0^{11}(\boldsymbol{q},\bar{r},m,g) - G_0^{11}(\boldsymbol{q},0,m,g)\right] + \frac{n-1}{6}\lambda\int_{\boldsymbol{q}}\left[G_0^{jj}(\boldsymbol{q},\bar{r},m,g) - G_0^{jj}(\boldsymbol{q},0,m,g)\right] . \quad (56)$$

As in Sec. III, we restrict our attention to $n = d = 4-\epsilon$. It suffices to set $n = 4$ in Eq. (56) to the order considered. The dimensionless vertex $\Gamma_{11}^{(2)}$ can now be written as

$$\Gamma_{11}^{(2)}\left(0;\frac{\bar{r}}{\kappa^2},\frac{m}{\kappa^2},\frac{g}{\kappa^2},\frac{\lambda}{\kappa^\epsilon}\right) = \frac{\bar{r}}{\kappa^2} + \frac{gN_{11}}{\kappa^2} + \frac{\lambda}{\kappa^\epsilon}\Sigma\left(\frac{\bar{r}}{\kappa^2},\frac{m}{\kappa^2},\frac{g}{\kappa^2}\right) , \quad (57)$$

with

$$\Sigma\left(\frac{\bar{r}}{\kappa^2},\frac{m}{\kappa^2},\frac{g}{\kappa^2}\right) = -\frac{1}{2}\left[A\left(\frac{\bar{r}}{\kappa^2}\right) + J\left(\frac{\bar{r}}{\kappa^2},\frac{m}{\kappa^2}\right)\right]\frac{\bar{r}}{\kappa^2} - \frac{1}{2}\left[\Delta J_1\left(\frac{\bar{r}}{\kappa^2},\frac{m}{\kappa^2},\frac{g}{\kappa^2}\right) + \Delta J_2\left(\frac{\bar{r}}{\kappa^2},\frac{m}{\kappa^2},\frac{g}{\kappa^2}\right)\right] . \quad (58)$$

The integrals $A(x)$ and $J(x,y)$ are well known and are given in Appendix B. The calculation of the quantities $\Delta J_{1,2}(x,y,z)$ is complicated and is sketched out in Appendix C. These perturbation contributions contain no divergences of the type $1/\epsilon$ which in fact confirms the statement concerning the pole structure of c_1 [cf. Eq. (44) above]. Therefore, the assumptions which lead to Eq. (53) for γ_{eff} are fulfilled and the equation itself can be used further. In doing this, the quantity S defined in Eq. (54) is represented as

$$S = S_0 + S_1 + S_2 , \quad (59)$$

where S_0 is the part containing the "usual" integrals A and J. For a system without dipole interactions ($g = 0$), one has, identically, $S_1 = S_2 = 0$. In this particular case,

$$S_0 = -\frac{\tau}{2S_d}\frac{\partial}{\partial\tau}\left[A(1) + J\left(1,\frac{m}{\tau}\right)\right] , \quad (60)$$

and with the integral J from (B6) one finds the result of Ref. 28, namely,

$$\gamma_{\text{eff}} = 1 + \left[\frac{1}{2} - \frac{1}{4}\frac{m}{\tau}\ln\left(1+\frac{\tau}{m}\right)\right]u\left(\frac{\sqrt{\tau}}{\kappa}\right) . \quad (61)$$

For the case $g \neq 0$, the calculation of S_1 and S_2 is described in some detail in Appendix C. One finally obtains

$$\gamma_{\text{eff}} = 1 + \left[-\frac{6a+9}{72y}\ln\left[\sqrt{y^2+y(a+1)+a}+\sqrt{y^2+y(a+1)}\right] - \frac{a}{6y}\ln(a+y) + \left(\frac{10a+3}{48y}\right)\ln a + \frac{9+6a}{72y} + \frac{3ay^3+(48a^2+4a)y^2+(46a^3+45a^2+1)y+a^4-2a^2+1}{72a^2\sqrt{y+a+1}\sqrt{y}\left[\sqrt{y+a+1}\sqrt{y}+\sqrt{(y+a)(y+1)}\right]} + \frac{-3ay^4+(24a^2-4a)y^3+(28a^3+21a^2+1)y^2+(a^4+12a^3-2a^2+1)y-6a^4-9a^3}{72a^2y\sqrt{(y+a)(y+1)}\left[\sqrt{y+a+1}\sqrt{y}+\sqrt{(y+a)(y+1)}\right]} - \frac{7a^3+7a^2+a+1}{72a^2y}E\left(\varphi,\frac{a-1}{a+1}\right) + \frac{3a^2+4a+1}{36ay}F\left(\varphi,\frac{a-1}{a+1}\right)\right]u\left(\frac{\sqrt{\tau}}{\kappa}\right) , \quad (62)$$

where the abbreviations

$$y = \frac{\tau}{g}, \qquad a = \frac{m}{g} , \quad (63)$$

and

$$\varphi = \arcsin\sqrt{\frac{y^2+y(a+1)}{y^2+y(a+1)+a}} \quad (64)$$

are used, while $F(\varphi,k)$ and $E(\varphi,k)$ are the elliptic integrals of the first and second kinds, respectively (see Appendix D or Ref. 52).

Equation (62) with $u(\rho)$ taken from Eq. (29) represents the full analytical solution to the crossover problem in easy-axis ferromagnets with dipolar interactions in terms of γ_{eff}. It simplifies considerably if the anisotropy and the dipolar interactions are equally strong, i.e., $m = g$, thus reducing the crossover problem to an effectively single-parameter one. The parameter a is then equal to 1, while the elliptic integrals are trivial and cancel each other because of the relation $E(\varphi,0) = F(\varphi,0)$. The effective exponent is then

$$\gamma_{\text{eff}} = 1 + \left[\frac{5}{24y} - \frac{1}{6y}\ln(1+y) - \frac{5}{24y}\ln\left[1+y+\sqrt{y(y+2)}\right] + \frac{1}{72}\frac{27+23y-3y^2-15y^{-1}}{1+y+\sqrt{y(y+2)}} + \frac{1}{72}\frac{92+52y+3y^2}{1+y+\sqrt{y(y+2)}}\sqrt{\frac{y}{y+2}}\right]u\left(\frac{\sqrt{\tau}}{\kappa}\right) , \quad (65)$$

which coincides with the result of a recent study of this particular case.[38]

The general result for γ_{eff} is plotted in Fig. 4 for some

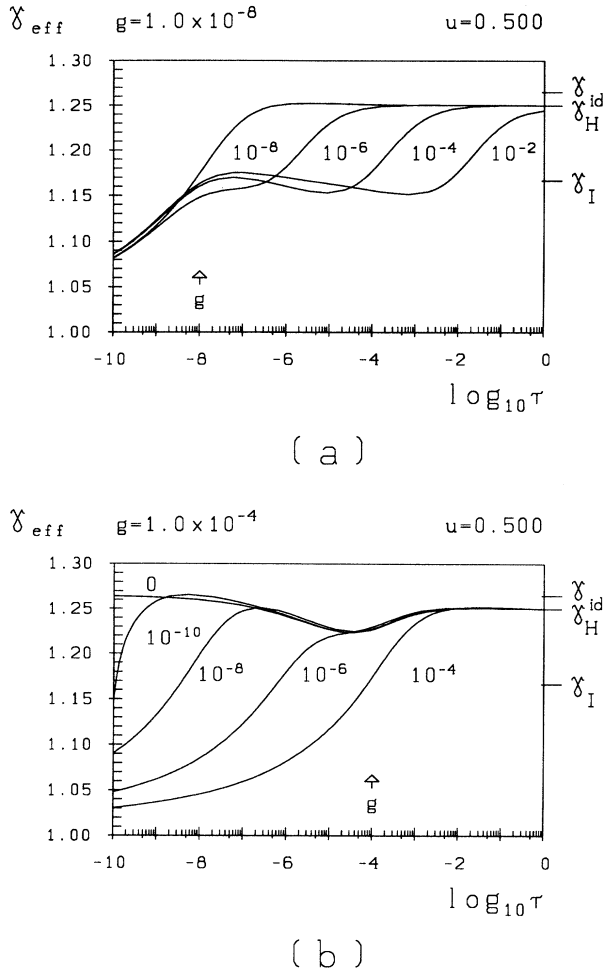

FIG. 4. The effective exponent γ_{eff} for $m \geq g$ (a) and for $m \leq g$ (b). The parameters are chosen as $u = u_H^* = 1/2$, $\kappa = 1$ and different values of m shown next to each curve. The curves with $m = 0$ and $m = 10^{-10}$ in (b) have been calculated using the expansion (68) up to the order $(m/\tau)^2$.

representative values of the parameters. In this context, it is helpful to recall the values of the asymptotic critical exponent γ characteristic of the four nontrivial fixed points (cf. Table I) which are indicated at the right margin of the figures.

The case with $m \geq g$ is presented in Fig. 4(a). For high temperatures $\tau \gg m, g$, γ_{eff} is equal to the Heisenberg exponent γ_H regardless of m and g. A crossover to Ising critical behavior $\gamma_H \to \gamma_I$ takes place for $\tau \approx m$, provided that $m \gg g$. As τ becomes smaller, there follows a second crossover to uniaxial dipolar critical behavior $\gamma_I \to \gamma_{\text{UD}}$. Asymptotically, for $\tau \to 0$, the effective exponent takes on the mean-field value of unity. This crossover transition is, however, very slow because of the logarithmic corrections to the mean-field behavior which come into play in this regime. As seen in Fig. 4(a), the γ_{eff} curves are nonmonotonic for $m \gg g$. Under the same condition, there exist two extrema, a minimum and a maximum. As the value of m decreases and approaches that of g, the first (Heisenberg-to-Ising) crossover is shifted to smaller temperatures and, besides, the extrema are wiped out. The successive crossovers overlap and a direct monotonic crossover from Heisenberg to uniaxial dipolar behavior takes place ($\gamma_H \to \gamma_{\text{UD}}$). Consequently, for $m \to g^+$ there is no range in the variable τ where Ising-like behavior shows up. For $m = g$, the crossover is a straightforward one.

The case with $m \leq g$ is depicted in Fig. 4(b). Heisenberg criticality dominates once again for $\tau \gg m, g$ with $\gamma_{\text{eff}} \approx \gamma_H$. For $m = 0$, one finds a single crossover $\gamma_H \to \gamma_{\text{ID}}$ to the isotropic dipolar value with a characteristic dip which has already been reported for this particular case.[27,30,31] The dip exists also for small values of anisotropy ($m \ll g$) without an appreciable change in its location. However small m might be, it brings about a second crossover $\gamma_{\text{ID}} \to \gamma_{\text{UD}}$ to the asymptotic uniaxial dipolar behavior which proceeds slowly with $\tau \to 0$ because of the logarithmic corrections. In this regime ($m \ll g$), the γ_{eff} curves exhibit a maximum and a minimum. The extrema and the successive crossover transients overlap for $m \to g^-$, indicating a unique direct crossover $\gamma_H \to \gamma_{\text{UD}} \to 1$. For $m = g$, finally, the situation is the same as in Fig. 4(a).

TABLE I. The coupling constant u^* and the exponent γ to $O(\epsilon^1)$ for the four nontrivial fixed points. The last column contains the estimate at $d = 3(\epsilon = 1)$. The quantity p is nonuniversal and is given in Eq. (77).

Heisenberg	$u_H^* = \epsilon/2$	$\gamma_H = 1 + \epsilon/4$	≈ 1.250
Ising	$u_I^* = 2\epsilon/3$	$\gamma_I = 1 + \epsilon/6$	≈ 1.167
Isotropic dipolar	$u_{\text{ID}}^* = 12\epsilon/17$	$\gamma_{\text{ID}} = 1 + 9\epsilon/34$	≈ 1.265
Uniaxial dipolar	$u_{\text{UD}}^* \to \infty$	$\gamma_{\text{UD}} = 1 + p/\lvert\ln\tau\rvert$	$\to 1$

C. Influence of κ and u

The result (62) for the effective exponent should be universal within the critical temperature region. Consequently γ_{eff} within the critical region has to be independent of the irrelevant parameter $u = u(1)$ which is connected to the bare coupling constant λ via Eq. (17c). Additionally, the influence of the free parameter κ which has been generated through the renormalization procedure has to be investigated. Below the influence of u and κ on the effective exponent γ_{eff} will be discussed and conditions for the range of the critical temperature region where the crossover function is believed to be universal will be given.

The terms in the square brackets of Eq. (62) are functions of the physical quantities τ, m, and g and the parameters u and κ enter only via the coupling constant $u(\rho)$ given in Eq. (29) which has to be investigated for $\rho = \sqrt{\tau}/\kappa$. We first consider the case of small anisotropy and dipolar parameters, i.e., $m \ll \kappa^2$ and $g \ll \kappa^2$. In this case the part of $u^{-1}(\sqrt{\tau}/\kappa)$ depending on the free parameters u and κ reads

$$\frac{\sqrt{\tau}}{\kappa}\left(\frac{1}{u} - \frac{1}{u_H^*}\right) + O\left(\frac{\sqrt{\tau m}}{\kappa^2}, \frac{\sqrt{\tau g}}{\kappa^2}\right) ,$$

with $u_H^* = 1/2$. The condition that the effective exponent should be independent of u and κ now results in the relation

$$\frac{\sqrt{\tau}}{\kappa}\left(\frac{1}{u}-\frac{1}{u_H^*}\right)+O\left(\frac{\sqrt{\tau m}}{\kappa^2},\frac{\sqrt{\tau g}}{\kappa^2}\right)\ll\frac{1}{u_H^*}\,. \tag{66}$$

For the critical temperature region it follows

$$\tau \ll \frac{\kappa^2 u^2}{(u-u_H^*)^2} \tag{67a}$$

and

$$\tau \ll \kappa^2\,, \tag{67b}$$

which has already been mentioned as Eq. (30). As discussed in Sec. III, κ and u are free parameters within the framework of renormalized-field theory and therefore the width of the critical region remains undetermined. The crossover theory is, however, meaningful only if the crossover transitions take place inside the critical region. It is then clear, in connection with Eq. (67b), that the case $m, g \ll \kappa^2$ discussed above is the most interesting one.

The influence of κ and u upon the effective exponent γ_{eff} is demonstrated in Fig. 5. The curves are plotted for $m = 10^{-8}$ and $g = 10^{-4}$ and different values of u. The solid curves correspond to $\kappa = 1$ and the curve for $u = u_H^* = 1/2$ is already known from Fig. 4(b). It is obvious from Fig. 5 that the value of u determines the width of the critical region and influences strongly the effective exponent outside the critical region. Inside the critical region given by Eq. (67a) the effective exponent γ_{eff} is independent of the choice of u as predicted above. The dashed curves in Fig. 5 correspond to $\kappa = 0.1$. According to Eq. (67b), the boundary of the critical region is shifted to lower values of the reduced temperature τ for smaller values of κ.

It must be mentioned that even with the choice $u = u_H^*$ the range of the critical region is not infinite. According to the flow equation (29), in the limit $\tau \to \infty$ we always find $u(\sqrt{\tau}/\kappa) \to 0$ which corresponds to the mean-field behavior with $\gamma_{\text{eff}} \to 1$. In the case of $u = u_H^*$ this effect results in a maximum of γ_{eff} found at $\tau \approx \kappa^2$. The maximum can be seen clearly in the dashed curve of Fig. 5 and has been discussed previously in the context of dipolar Ising systems.[34] It has to be pointed out that the locus of the maximum is not part of the universal crossover function since it depends on the choice of the free parameter κ. However, within a phenomenological interpretation of the theory, it is possible to choose κ in such a way that this locus fits experimental data. This has been done in Ref. 34 resulting in $\kappa = 1$ for the dipolar Ising ferromagnet $LiTbF_4$.

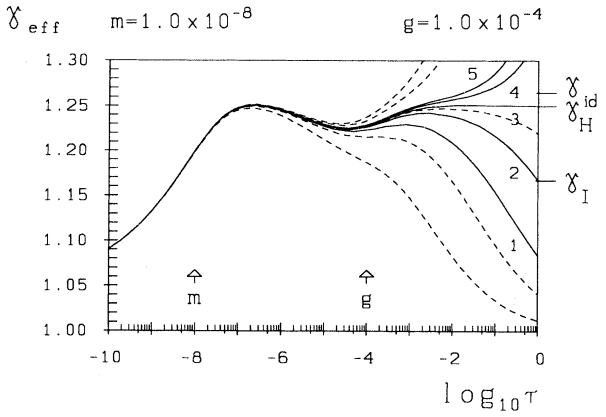

FIG. 5. The effective exponent γ_{eff} for $m = 10^{-8}$ and $g = 10^{-4}$. We used $u = k/6$ with k indicated next to each curve. The solid curves correspond to $\kappa = 1$ and the dashed curves correspond to $\kappa = 0.1$.

V. LIMITING CASES OF THE GENERAL TWO-PARAMETER STUDY

Now that one has gained an impression as to what features are latent in the general result (62) for γ_{eff}, it is worthwhile to discuss analytically the important limiting cases which substantiate unambiguously the correctness of the procedure and the richness of the result. In doing this systematically, important new results concerning the asymptotic logarithmic corrections are derived.

A. $\tau \gg m$

Uniaxial anisotropy cannot be "felt" in this regime. Depending on the ratio between τ and g, one obtains isotropic short-range (Heisenberg) or isotropic dipolar behavior corresponding to $n = d$.

In Eq. (62), $\tau \gg m$ is equivalent to $y \gg a$. Expanding in the small parameter a and surmounting the difficulties which result from the singular behavior of $F(\varphi, k)$ for $a = 0$, $\varphi = \pi/2$, one uses (D4) and (D5) to obtain

$$\begin{aligned}\gamma_{\text{eff}} = 1 + \Bigg[&\frac{4y-\ln(y+1)}{8y}+\frac{5}{24y}\,a\ln a\\ &-\frac{1}{72}\left(15\ln y+3\ln(y+1)+6\ln 2-\frac{7y}{y+1}\right)\frac{a}{y}\\ &+O\left(\left(\frac{a}{y}\right)^2, a^2\ln a\right)\Bigg]u\left(\frac{\sqrt{\tau}}{\kappa}\right)\,.\end{aligned} \tag{68}$$

When the anisotropy is switched off ($m = 0$ and, hence, $a = 0$),

$$\gamma_{\text{eff}} = 1+\frac{1}{8}\left[4-\frac{g}{\tau}\ln\left(1+\frac{\tau}{g}\right)\right]u\left(\frac{\sqrt{\tau}}{\kappa}\right)\,, \tag{69}$$

which agrees with the result of Ref. 31. Taking the corresponding limit for $u(\rho)$ in Eq. (29), one finds that (i) for $\tau \gg g$, $\gamma_{\text{eff}} \to 1 + u(\sqrt{\tau}/\kappa)/2 = 1 + \epsilon/4 = \gamma_H$; (ii) for $\tau \ll g$, $\gamma_{\text{eff}} \to 1 + 9\epsilon/34 = \gamma_{\text{ID}}$ (Refs. 7, 15) (cf. Table I).

B. $m \to \infty$

In this regime the system behaves like an Ising system with a single order-parameter component ($n = 1$). The

infinite anisotropy is given by $m \gg g, \tau$ which implies that the quantities $G_0^{jj}(\boldsymbol{q})$, ΔJ_2, and S_2 from Eqs. (56), (58), and (59) vanish simultaneously. Now one expands the remaining part of S in powers of $a^{-1} = g/m$. It follows that

$$\gamma_{\text{eff}} = 1 + \left[\frac{1-y}{4} + \frac{y^2+2y+11/8}{4(y+1)} \sqrt{\frac{y}{y+1}} - \frac{1}{8y} \ln\left(\sqrt{y+1}+\sqrt{y}\right) + \frac{1}{16y} - \frac{y+1/4}{8\left(\sqrt{y+1}+\sqrt{y}\right)} \left(\frac{1+2/y}{\sqrt{y+1}} + \frac{1}{\sqrt{y}}\right) + \frac{3}{32(y+1)^{3/2}\sqrt{y}} + O\left(\frac{1}{a}\right) \right] u\left(\frac{\sqrt{\tau}}{\kappa}\right) . \quad (70)$$

Taking once again the proper limits for $u(\rho)$ in Eq. (29), one finds from Eq. (70) that (i) for $\tau \gg g$ $(y \to \infty)$, $\gamma_{\text{eff}} \to 1 + u(\sqrt{\tau}/\kappa)/4 = 1 + \epsilon/6 = \gamma_I$; (ii) for $\tau \ll g$ $(y \to 0)$,

$$\gamma_{\text{eff}} = 1 + \left[\frac{1}{3}\sqrt{\frac{\tau}{g}} - \frac{1}{4}\left(\frac{\tau}{g}\right) + O\left(\left(\frac{\tau}{g}\right)^{\frac{3}{2}}\right) \right] u\left(\frac{\sqrt{\tau}}{\kappa}\right) \quad (71)$$

and

$$u\left(\frac{\sqrt{\tau}}{\kappa}\right) \approx -\frac{4}{3}\sqrt{\frac{g}{\tau}} \frac{1}{\ln\tau - \ln\kappa^2} , \quad (72)$$

which is in agreement with previous calculations for this case.[34] The critical region is attained for $\rho \ll 1$ or $\tau \ll \kappa^2$. Then

$$\gamma_{\text{eff}} \approx 1 + \frac{4}{9}\frac{1}{|\ln\tau|} \quad (73)$$

and $\gamma_{\text{eff}} \to 1$ as $\tau \to 0$. This is the typical mean-field behavior with logarithmic corrections in dipolar Ising systems. The known result for the leading term in the susceptibility of such systems is of the form

$$\chi_{11}^{-1} \sim \tau |\ln\tau|^{-p} \quad (74)$$

and, hence,

$$\gamma_{\text{eff}} = 1 + p\frac{1}{|\ln\tau|} . \quad (75)$$

According to Eq. (73), the "logarithmic" exponent p which follows from our general result equals 4/9, while it has been reported to be 1/3 in all previous studies of this aspect of criticality in dipolar Ising systems.[16–18,34,35] The seeming discrepancy is due to the fact that the integrals involved in Σ [Eq. (58)] were previously calculated directly at $d = 3$ in contrast to $d = 4 - \epsilon$ in the present work. In fact, if one performs an ϵ expansion in, e.g., Eq. (5.7) of Ref. 34, one obtains $p = 4/9$ in accordance with what we find.

C. $\tau \to 0$: The general nonuniversal "logarithmic" exponent p

Arbitrary m and g can be considered in this limit. One expands the expression in the square brackets of Eq. (62) in powers of $y = \tau/g$ to find that

$$\gamma_{\text{eff}} = 1 + \left[\frac{1}{3}\sqrt{\frac{a+1}{a}}\sqrt{y} - \frac{a+1}{4a}y + O\left(y^{3/2}\right) \right] u\left(\frac{\sqrt{\tau}}{\kappa}\right) . \quad (76)$$

It follows from the last equation when examined together with Eq. (29) for $u(\rho)$ that in the critical region $(\tau \ll \kappa^2)$ the leading term of the effective critical exponent is given by Eq. (75) with[41]

$$p = \frac{4}{9} \frac{\sqrt{1+g/m}}{1 + \frac{17}{18}\sqrt{g/m} - \frac{11}{18}\sqrt{g/(m+g)}} . \quad (77)$$

The implication of the last equation is that the true asymptotic critical behavior of the easy-axis susceptibility is of the mean-field type with logarithmic corrections as in Eq. (74) with the "logarithmic" exponent p modified by the simultaneous account of anisotropy and dipolar interactions. The limiting cases of extreme anisotropy $(p = 4/9)$ and of vanishing anisotropy $(p = 8/17)$ derive from Eq. (77) by taking $g/m \to 0$ and $g/m \to \infty$, respectively. It is to be seen that the "logarithmic" exponent is a quantity which depends explicitly on the values of the material parameters m and g, in contrast to the universal critical exponents which depend on the dimensionality of spin and space only.

VI. DISCUSSION

A. Parameters

A discussion of the parameters m, g, and τ appearing in Eq. (62) is in order if one wants to use the result for γ_{eff}. The relation of the parameters of the effective Hamiltonian (2) to microscopic quantities was given in Refs. 7, 13. There the discussion was limited to cubic lattices. The applications of our model which will be discussed below concern noncubic lattices and the more complicated case of compounds with different magnetic atoms. However, the relations of Refs. 7, 13 will be used since they are the simplest possible approximation and we are only interested in an order-of-magnitude estimate for the parameters. It was found that

$$r = s_1 k_B (T - T_0)/\tilde{J} , \quad (78a)$$

$$g = 2a_1 G/\tilde{J}a^d , \quad (78b)$$

$$m = c(J_1 - J_j)/\tilde{J} . \quad (78c)$$

The abbreviations

$$\tilde{J} = \frac{a^2 c J_1}{2d} - \frac{2a_4 G}{a^{d-2}} \tag{79}$$

and $s_1 = 3/S(S+1)$ have been used. S is the spin quantum number, a is the lattice constant, c is the number of nearest neighbors, and

$$T_0 = \frac{1}{s_1 k_B}\left(cJ_1 + \frac{2a_3 G}{a^d}\right) \tag{80}$$

is the mean-field critical temperature, while the constants a_1, a_3, and a_4 for cubic lattices are given in Ref. 7. G represents the dipolar coupling constant which reads $G = \mu_0 (g_s \mu_B)^2 / 8\pi$ in SI and $G = (g_s \mu_B)^2 / 2$ in the cgs system. g_s is the Landé factor and μ_B is Bohr's magneton. J_1 is the exchange integral which couples the easy-axis spin components, while $J_j (J_j < J_1)$ couples the spin components in the transverse directions $1 < j \leq n$. The anisotropy of the spin-rescaling factor $\tilde{J}$ which would formally lead to an anisotropic $\lambda_{\alpha\beta}$ in the fourth-order term in Eq. (2) is neglected in the present paper. It leads to the emergence of irrelevant quantities only.[13,14]

The quantities defined in Eqs. (78) have the dimension of inverse length squared $(1/L^2)$. Since it is more convenient to discuss the crossover scheme using dimensionless coupling constants, all parameters can be scaled by $\omega^2 = s_1 k_B T_0 / \tilde{J}$. One obtains

$$t_{\mathrm{MF}} = \frac{r}{\omega^2} = \frac{T - T_0}{T_0} , \tag{81}$$

which is the reduced temperature in the mean-field approximation. Considering the relation $a_1/a^d = 4\pi/v_a$ which is valid for all cubic lattices,[7] with v_a being the volume per atom, one obtains the dimensionless dipolar coupling constant

$$g_0 = \frac{g}{\omega^2} = \frac{\mu_0 S(S+1)(g_s \mu_B)^2}{3 k_B T_0 v_a} , \tag{82}$$

with the parameters given in the SI system. The coupling constant g_0 is related to the shift amplitude $\hat{g}$ discussed in Ref. 6 via $g_0 = 3\hat{g}$ as follows from Eq. (80) with $a_3 = a_1/3$. With $T_0 \approx cJ_1/s_1 k_B$, it follows then for the anisotropy parameter

$$m_0 = \frac{m}{\omega^2} \approx \frac{J_1 - J_j}{J_1} \approx \frac{T_0 - T_0'}{T_0} . \tag{83}$$

T_0' is the "critical temperature" of the perpendicular direction which can easily be determined experimentally.[39,40]

The shift of the critical temperature from the mean-field value was introduced in Eq. (18) resulting in a new temperature scale $\bar{r}$ with $\bar{r}/\omega^2 = (T - T_c)/T_0$ with the real critical temperature T_c. Typically, for ferromagnets $T_c \approx 0.7 T_0$ (Refs. 6, 53, 54) and, hence, $\bar{r}/\omega^2 \approx (T - T_c)/T_c$. The renormalized temperature scale τ is related to $\bar{r}$ by Eqs. (17b) and (19b). The renormalization factor $Z_\phi^2 = 1 + c_1 u$ is a constant of order unity, because $u \sim \epsilon$ and $c_1 \sim 1/\epsilon$ according to Eq. (44). Consequently, it is plausible to make the identification

$$\frac{\tau}{\omega^2} \approx t = \frac{T - T_c}{T_c} , \tag{84}$$

where t is the usual reduced temperature. Since the parameters enter Eq. (62) as the ratios τ/g and m/g only, one is justified to make the substitutions

$$m \to m_0 , \quad g \to g_0 , \quad \text{and} \quad \tau \to t . \tag{85}$$

All results will then hold in the form given so far, provided that the additional substitution $\kappa \to \bar{\kappa}$ with $\bar{\kappa} = \kappa/\omega$ is carried out in Eq. (29). In the critical region, however, the effective exponent must be independent of the choice of the arbitrary momentum κ or $\bar{\kappa}$. This is the ground to insert the dimensionless quantities g_0 and m_0 for g and m below; accordingly, τ is then interpreted as the experimental temperature scale t.

B. Gd and $Fe_{14}Nd_2B$

Since in Gd the total orbital momentum of the f electrons is zero $(L = 0)$, no crystal-field effects are expected. However, a small magnetocrystalline anisotropy is observable near T_c (Ref. 55) and is attributed to the effect of dipolar interactions on the spins located on a lattice with a nonideal c/a ratio.[56] The coupling constants g_0 and m_0 can easily be estimated using Eqs. (82) and (83) in the case of Gd. The mean-field critical temperature T_0 is determined by the approximate relation[6] $T_0 \approx T_c/\theta$ with $\theta = 0.68$–0.80 for $S = 1/2$ to ∞. For Gd, taking $T_c = 293.6$ K,[56] $\theta = 0.8$, $S = 7/2$, $g_s = 2$, and $v_a = 33.0$ Å^3, one obtains $g_0 = 1.3 \times 10^{-2}$. With the paramagnetic Curie temperatures $T_0 = 295.5$ K and $T_0' = 294.0$ K,[55] it follows that $m_0 = 5.1 \times 10^{-3}$ for the anisotropic coupling constant. These values are not in perfect agreement either with the values of $g_0 = 3\hat{g} = 4.0 \times 10^{-3}$ and $m_0 = 1.4 \times 10^{-4}$ of Ref. 57 or with $g_0 = 1.6 \times 10^{-2}$ and $m_0 = 2.5 \times 10^{-4}$ obtained in Ref. 56 by a somewhat different method. Since an order-of-magnitude estimate of the parameters g_0 and m_0 is sufficient for the interpretation of γ_{eff}, the different approaches and their results are not discussed here in further detail.

The volume per atom, v_a, for $Fe_{14}Nd_2B$ is approximated with the help of the relation $v_a = \mu_B g_s S / M_s(0)$. With $S = 1$, which is a plausible approximation for iron, $g_s = 2$, and with a saturation magnetization $\mu_0 M_s(0) = 1.86$ T at $T = 0$ K,[58] one obtains $v_a = 12.5$ Å^3. From Eq. (82), $T_c = 583.7$ K (Ref. 40), and $\theta = 0.7$ it follows that $g_0 = 2.0 \times 10^{-3}$. Since the "critical temperature" of the perpendicular direction T_0' has not been determined experimentally,[39] we estimate m_0 via the relation[40]

$$m_0 = \frac{K_1'}{T_0 A'} . \tag{86}$$

Taking the experimental values[46] of $K_1' = 1.20$ for the anisotropy constant, $A' = 0.171$ K^{-1} for the Landau parameter, and $T_0 \approx T_c$, one finds $m_0 = 1.2 \times 10^{-2}$ for the anisotropic coupling constant.

Gadolinium is a material with a comparatively low anisotropy $(m_0 < g_0)$, while $Fe_{14}Nd_2B$ represents the op-

posite case with high anisotropy ($m_0 > g_0$). Hence, the results for Gd should be discussed according to the right-hand side of Fig. 1 corresponding to a crossover behavior via the isotropic dipolar fixed point, while the behavior of $Fe_{14}Nd_2B$ should follow the scheme of the left-hand side of Fig. 1. In Fig. 6, the effective exponent γ_{eff} is plotted for the cases of Gd and $Fe_{14}Nd_2B$ with the parameters m_0 and g_0 estimated above and for different values of u. Surprisingly, one observes almost identical critical behavior in both exemplary cases. For $u = u_H^* = 1/2$, which corresponds to the widest extension of the critical region according to Eqs. (67), the curves indicate a direct transition from the Heisenberg exponent γ_H to the mean-field behavior with logarithmic corrections $\gamma_{\text{eff}} \to 1$. This should be attributed to the proximity of m_0 and g_0 in both cases: It does not allow the intermediate critical behavior to show up.

Experimental results for the exponent γ of Gd and $Fe_{14}Nd_2B$ are listed in Table II. For the case of Gd, we

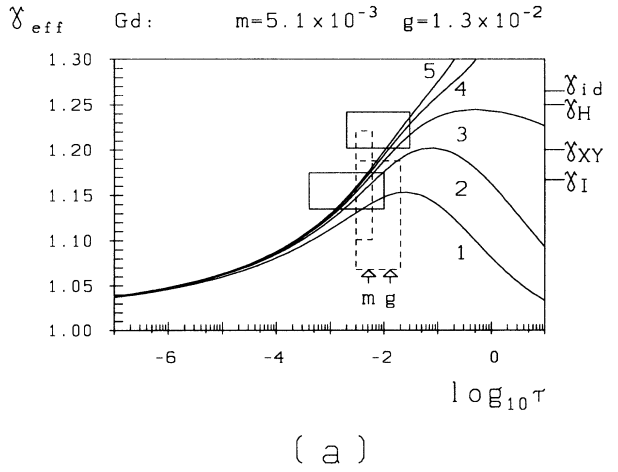

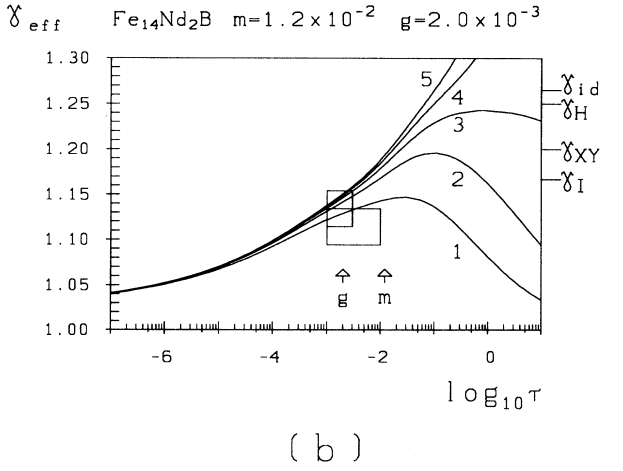

FIG. 6. The effective exponent γ_{eff} calculated with the material parameters of Gd (a) and $Fe_{14}Nd_2B$ (b). The curves were obtained using $\kappa = 1$ and $u = k/6$ with the value of k indicated next to each curve. The solid rectangles correspond to the experimental results of Refs. 56, 57, 39 and the dashed rectangles to those of Ref. 59.

TABLE II. Recent experimental results for the exponent γ in Gd and $Fe_{14}Nd_2B$.

Method	Range of $\lvert t\rvert$	γ	Error	Ref.
	Gd			
ac susceptibility	2×10^{-3}–3×10^{-2}	1.33	±0.02	57
ac susceptibility	4×10^{-4}–1×10^{-2}	1.23	±0.02	56
Arrott plot	3×10^{-3}–6×10^{-3}	1.24	±0.06	59
Scaling plot	3×10^{-3}–2×10^{-2}	1.19	±0.06	59
	$Fe_{14}Nd_2B$			
Arrott plot	1×10^{-3}–3×10^{-3}	1.20	±0.02	39
Scaling plot	1×10^{-3}–1×10^{-2}	1.17	±0.02	39

present, apart from the results of recent susceptibility studies,[56,57] some novel data[59] obtained by analysis of the magnetization curves in the ferromagnetic ($T < T_c$) and in the paramagnetic ($T > T_c$) regions. The experimental technique there is the same as applied for the investigation of $Fe_{14}Nd_2B$.[39] It is obvious from Table II that there is a remarkable difference between the γ values reported for Gd by different authors which exceeds the estimated experimental error. The situation becomes even more confusing when earlier data, summarized in Ref. 60, is considered. According to the crossover scheme discussed above, Gd and $Fe_{14}Nd_2B$ should exhibit mean-field behavior $\gamma_{\text{eff}} \to 1$ in the asymptotic limit $t \to 0$. Consequently, the experimental values of γ do not represent asymptotic exponents and have to be discussed as effective exponents valid in the investigated temperature range $t_{\min} < |t| < t_{\max}$. The corresponding value of $t_{\min}$ was explicitly given in the case of the susceptibility studies[56,57] and was calculated from the minimum temperature step between two isotherms in the case of the magnetization studies.[39,59]

A direct comparison between theoretical and experimental results is hampered by the low order of the calculation. In Table III, the one-loop values of γ are compared with those exponents which are currently accepted to be the most accurate estimates in three dimensions. There is considerable difference between the numerical values of the two sets of data. It must, however, be emphasized that already the one-loop order provides for a reliable qualitative picture of the critical behavior. This statement was confirmed by a lot of previous studies[23,24,26,27,37] of crossover phenomena in anisotropic or dipolar models. It turned out that the shape of the crossover function remains almost unchanged when going from the first order to higher orders in ϵ or to series expansions. The only substantial difference between the different orders of calculation was a nearly homogeneous

TABLE III. The critical exponent γ obtained to the first order of the ϵ expansion compared to the results which are believed to be the most accurate at $d = 3$ (Refs. 3, 15).

Model		$O(\epsilon)$	$d = 3$
Heisenberg	$(n = d)$	1.250	1.387
XY	$(n = 2)$	1.200	1.316
Ising	$(n = 1)$	1.167	1.240
Isotropic dipolar	$(n = d)$	1.265	1.372

shift of the exponents associated with the various fixed points. To give a qualitative interpretation of our result for γ_{eff} of Gd, we first note that all the experimental data shown in Table II were obtained in the temperature range of $4 \times 10^{-4} < |t| < 3 \times 10^{-2}$. Examining Fig. 6(a) over this interval, it should be expected that the effective-exponent values are located in an interval from a little bit below the Ising exponent γ_I up to somewhat above the XY exponent γ_{XY}. Looking at Table II again, it is satisfying to see that the experimental results are indeed found between a maximum value of $\gamma = 1.33$ which is close to the "exact" value of $\gamma_{XY} = 1.316$ of the XY exponent and a minimum value of $\gamma = 1.19$ which is below the "exact" value of $\gamma_I = 1.240$ of the Ising exponent. For $Fe_{14}Nd_2B$, an effective exponent located below the Ising exponent γ_I is to be expected in the experimentally investigated interval of $1 \times 10^{-3} < |t| < 1 \times 10^{-2}$ as suggested by Fig. 6(b). The results shown in Table II are in agreement with this prediction and lie below the value of $\gamma_I = 1.240$.

Finally, we want to interpret our results in a more quantitative, still purely phenomenological way. Starting from the observation of previous studies that the calculation to higher orders in ϵ is compatible with a mere shift of the exponents for the different fixed points, we characterize this shift by a phenomenological equation. Considering the data of Table III, the approximate equation

$$\gamma_{1\text{ loop}} = 0.672\,(\gamma_{\text{exact}} - 1) + 1 \tag{87}$$

is obtained under the constraint that the mean-field exponent is independent of the order of the calculation (i.e., $\gamma_{1\text{ loop}} = \gamma_{\text{exact}} = 1$). Here $\gamma_{1\text{ loop}}$ represents the result of order ϵ and γ_{exact} stands for the best available estimate. The experimental exponents of Table II are inserted as γ_{exact} into the above equation and the resulting values of $\gamma_{1\text{ loop}}$ are interpreted as the experimental data scaled down to the one-loop order. These "shift-corrected" experimental exponents are plotted together with our theoretical curves shown in Fig. 6. Each data point is represented by a rectangle whose height corresponds to the experimental error and whose length corresponds to the investigated temperature region. We obtain a satisfactory agreement between theoretical and experimental results in both cases of Gd and $Fe_{14}Nd_2B$ as displayed in Fig. 6.

To summarize, we have shown that unexplained or contradictory experimental results for critical exponents can be understood if they are interpreted as effective exponents of the investigated temperature region and are compared to crossover calculations. Due to the low order of our calculation, the comparison is, more or less, a qualitative one. A study up to the order of ϵ^2 would be sufficient to directly map experimental onto theoretical data. There is, however, little hope that this can be done in the complicated case of anisotropic dipolar ferromagnets discussed in the present paper.

ACKNOWLEDGMENTS

Y.M. acknowledges the hospitality of MPI für Metallforschung in Stuttgart, financial support from the Alexander-von-Humboldt Foundation, and support under Contract No. F205/BSF.

APPENDIX A: INTEGRALS OF $\Gamma^{(4)}_{1111}$

The integrals required for the calculation of $\Gamma^{(4)}_{1111}$ according to Eq. (23) are

$$I_\alpha(r,m,g) = \frac{S_{d-1}}{2\pi}\int_0^\infty \int_0^\pi q^{d-1}\sin^{d-2}\theta\, X_\alpha(\theta,q)\,\mathrm{d}\theta\mathrm{d}q, \tag{A1}$$

with

$$X_1(\theta,q) = \frac{2g\left(r+m+q^2\right)\cos^2\theta}{\left(r+q^2\right)^2\Omega}, \tag{A2a}$$

$$X_2(\theta,q) = \left[\frac{g\left(r+m+q^2\right)\cos^2\theta}{\left(r+q^2\right)\Omega}\right]^2, \tag{A2b}$$

$$X_3(\theta,q) = \frac{1}{d-1}\left[\frac{g\sin\theta\cos\theta}{\Omega}\right]^2, \tag{A2c}$$

$$X_4(\theta,q) = \frac{1}{(d-1)}\cdot\frac{2g\left(r+q^2\right)\sin^2\theta}{\left(r+m+q^2\right)^2\Omega}, \tag{A2d}$$

$$X_5(\theta,q) = \frac{1}{(d-1)(d+1)}\left[\frac{g\left(r+q^2\right)\sin^2\theta}{\left(r+m+q^2\right)\Omega}\right]^2, \tag{A2e}$$

and

$$\Omega = \left(r+m+q^2\right)\left(r+g+q^2\right) - gm\sin^2\theta\,. \tag{A3}$$

Apart from the integrals I_α, two simple integrals

$$I_0(r) = \int_{\boldsymbol{q}} \frac{1}{\left(r+q^2\right)^2} \tag{A4}$$

and

$$\bar{I}_0(r,m) = \int_{\boldsymbol{q}} \frac{1}{\left(r+m+q^2\right)^2} \tag{A5}$$

are involved in Eq. (23). Within the framework of the GMS scheme, the knowledge of only the diverging parts of the integrals suffices to carry out the renormalization of the vertex functions. Divergences in the integrals appear in the case $d \to 4$, i.e., $\epsilon \to 0$, as well as in the cases $m \to \infty$ and $g \to \infty$. According to Eq. (B2), the divergent parts of (A4) and (A5) read

$$I_0^{\text{div}}\left(\frac{r}{\kappa^2}\right) = \frac{S_d}{\epsilon} \tag{A6}$$

and

$$\bar{I}_0^{\text{div}}\left(\frac{r}{\kappa^2},\frac{m}{\kappa^2}\right) = \frac{S_d}{\epsilon} - \frac{S_d}{2}\ln\left(\frac{r+m}{\kappa^2}\right). \tag{A7}$$

The calculation of I_1 will be discussed in some detail as an example for the integrals $I_1 - I_5$. The θ integration can be performed by means of the substitution $x = \sin^2\theta$ and Eq. (3.181) of Ref. 61:

$$\int_0^1 x^{b-1}(1-x)^{c-b-1}(1-xz)^{-a}\,dx = B(b,c-b)\,F(a,b;c;z)\ , \quad \text{(A8)}$$

which is valid for $\mathrm{Re}(b) > 0$, $\mathrm{Re}(c-b) > 0$, and $|z| < 1$. $F(a,b;c;z)$ is the hypergeometric function.[52] The usual abbreviation

$$B(x,y) = \Gamma(x)\,\Gamma(y)/\Gamma(x+y) \quad \text{(A9)}$$

has also been used. One makes use of the series representation of the hypergeometric function[52] with the result

$$I_1(r,m,g) = \frac{S_{d-1}}{2\pi}\Gamma\left(\frac{3}{2}\right)\sum_{n=0}^{\infty}\frac{\Gamma\left(\frac{d-1}{2}+n\right)}{\Gamma\left(\frac{d}{2}+1+n\right)}\int_0^{\infty} q^{d-1}\frac{2g\,(gm)^n}{(r+q^2)^2\,(r+g+q^2)^{n+1}\,(r+m+q^2)^n}\,dq\ . \quad \text{(A10)}$$

Each term of the sum is finite in the limit $d \to 4$. Since the integrals have to be calculated to the order ϵ^0, it is sufficient to set $\epsilon = 0$ or $d = 4$ in Eq. (A10). The sum is rewritten as

$$I_1 = I_1^0 + I_1^{\infty}\ , \quad \text{(A11)}$$

with the I_1^0 being the first term ($n = 0$). For this term it follows that

$$I_1^{0,\mathrm{div}}(r,m,g) = \frac{S_d}{4}\ln(r+g)\ . \quad \text{(A12)}$$

The terms of the sum (A10) with $n > 0$ are integrated by the standard method using the "Feynman-trick."[48,50] This introduces two further integrations over x_1 and x_2. The result is

$$I_1^{\infty}(r,m,g) = \frac{S_d}{2}\sum_{n=1}^{\infty}\frac{g\,(gm)^n\,\Gamma(2n+1)\,\Gamma(2n+2)}{\Gamma(n+1)\,\Gamma(n)\,\Gamma(n+3)\,4^n\Gamma(n+1)}\int_0^1\int_0^1\frac{x_1^n x_2^{n-1}(1-x_1-x_2)}{[r+x_1 g+x_2 m]^{2n+1}}dx_1 dx_2\ . \quad \text{(A13)}$$

It is straightforward to obtain the relation

$$\int\frac{x^m}{(gx+a)^p}dx = -\left[\sum_{k=0}^{\alpha}\frac{m!\,(p-2-k)!}{(m-k)!\,(p-1)!}\,\frac{x^{m-k}}{g^{k+1}\,(a+gx)^{p-1-k}}\right] + \begin{cases} \frac{-m!\,(p-m-2)!}{(p-1)!\,g^{m+1}\,(a+gx)^{p-m-1}} & \text{for } p-m>1, \\ \frac{1}{g^{m+1}}\ln(gx+a) & \text{for } p-m=1, \\ \frac{m!}{(p-1)!\,g^m}\left[x-\frac{a}{g}\ln(gx+a)\right] & \text{for } p-m=0, \end{cases} \quad \text{(A14)}$$

by partial integration. The upper limit of the sum is $\alpha = m-2$ for $p-m=0$ and $\alpha = m-1$ for $p-m>0$. To integrate the terms of the sum (A13), Eq. (A14) has to be applied twice, leading to a triple sum of complicated structure. However, within the framework of the GMS scheme, one is only interested in the diverging parts of the sum. It turns out that only logarithmic divergences appear for $m \to \infty$ or $g \to \infty$. Additionally, contributions of the type

$$\frac{1}{g}\left[\ln(r+m+g) - \ln(r+m)\right]$$

can be neglected, since they are finite in both limiting cases. For the divergent part of (A13) one obtains

$$I_1^{\infty,\mathrm{div}}(r,m,g) = -\frac{S_d}{2}\left[\sum_{n=1}^{\infty}\frac{(2n+1)!}{(n+2)!n!4^n}\right] \times[\ln(r+m+g) - \ln(r+m) - \ln(r+g)]\ . \quad \text{(A15)}$$

The infinite sum in the square brackets can be calculated using Eq. (5.2.13.12) of Ref. 62. With (A11) and (A12), the divergent part of I_1 finally reads

$$I_1^{\mathrm{div}}\left(\frac{r}{\kappa^2},\frac{m}{\kappa^2},\frac{g}{\kappa^2}\right) = S_d\ln\left(\frac{r+g}{\kappa^2}\right) - \frac{3}{4}S_d\left[\ln\left(\frac{r+m+g}{\kappa^2}\right) - \ln\left(\frac{r+m}{\kappa^2}\right)\right]\ . \quad \text{(A16)}$$

The calculation of I_2 can be performed along the same lines. It follows that

$$I_2^{\mathrm{div}}\left(\frac{r}{\kappa^2},\frac{m}{\kappa^2},\frac{g}{\kappa^2}\right) = \frac{S_d}{2}\ln\left(\frac{r+g}{\kappa^2}\right) - \frac{7}{16}S_d\left[\ln\left(\frac{r+m+g}{\kappa^2}\right) - \ln\left(\frac{r+m}{\kappa^2}\right)\right]\ . \quad \text{(A17)}$$

In calculating I_3–I_5, one finds that a contribution to the divergent part arises only from the $n = 0$ term in the series representation analogous to Eq. (A10). Consequently, no sums have to be calculated and one obtains

$$I_3^{\mathrm{div}}\left(\frac{r}{\kappa^2},\frac{m}{\kappa^2},\frac{g}{\kappa^2}\right) = \frac{S_d}{48}\left[\ln\left(\frac{r+m+g}{\kappa^2}\right)-\ln\left(\frac{r+m}{\kappa^2}\right)\right] \quad \text{(A18)}$$

and

$$\frac{1}{12}I_4^{\mathrm{div}} = I_5^{\mathrm{div}} = I_3^{\mathrm{div}} \ . \quad \text{(A19)}$$

One can calculate the vertex function $\Gamma^{(4)}_{1111}$ at $\boldsymbol{k} = 0$ by inserting Eqs. (A6), (A7), and (A16)–(A19) into Eq. (23).

APPENDIX B: SOME INTEGRALS IN DIMENSIONAL REGULARIZATION

The integrals given below can be calculated via standard methods[48,50] and are listed here to ensure self-sufficiency of the present study. The calculation of the four-point function in Appendix A requires the integral

$$I_0\left(\frac{\tau}{\kappa^2}\right) = \int_{\boldsymbol{q}} \frac{1}{\left(q^2+\frac{\tau}{\kappa^2}\right)^2} \ , \quad \text{(B1)}$$

whose ϵ expansion is

$$I_0\left(\frac{\tau}{\kappa^2}\right) = \frac{S_d}{\epsilon} - \frac{S_d}{2}\left[1+\ln\left(\frac{\tau}{\kappa^2}\right)\right] + O(\epsilon) \ . \quad \text{(B2)}$$

For the calculation of the susceptibility according to Eq. (58), one needs to know the two integrals

$$A\left(\frac{\tau}{\kappa^2}\right) = \int_{\boldsymbol{q}} \frac{1}{q^2\left(q^2+\frac{\tau}{\kappa^2}\right)} \ , \quad \text{(B3)}$$

whose ϵ expansion is

$$A\left(\frac{\tau}{\kappa^2}\right) = \frac{S_d}{\epsilon} - \frac{S_d}{2}\ln\left(\frac{\tau}{\kappa^2}\right) + O(\epsilon) \ , \quad \text{(B4)}$$

and

$$J\left(\frac{\tau}{\kappa^2},\frac{m}{\kappa^2}\right) = \int_{\boldsymbol{q}} \frac{1}{\left(q^2+\frac{m}{\kappa^2}\right)\left(q^2+\frac{\tau+m}{\kappa^2}\right)} \ , \quad \text{(B5)}$$

resulting in

$$J\left(\frac{\tau}{\kappa^2},\frac{m}{\kappa^2}\right) = \frac{S_d}{\epsilon} - \frac{S_d}{2}\left[\left(1+\frac{m}{\tau}\right)\ln\left(\frac{\tau+m}{\kappa^2}\right) - \left(\frac{m}{\tau}\right)\ln\left(\frac{m}{\kappa^2}\right)\right] + O(\epsilon) \ . \quad \text{(B6)}$$

As usual, the abbreviation

$$S_d = 2\Big/(4\pi)^{\frac{d}{2}}\,\Gamma\left(\frac{d}{2}\right) \quad \text{(B7)}$$

has been used.

APPENDIX C: INTEGRALS OF χ_{11}^{-1}

To find the inverse susceptibility χ_{11}^{-1} from Eqs. (32), (37), (57), and (58), one must calculate the quantities

$$\Delta J_1 = J_1(r,m,g) - J_1(0,m,g) \ , \quad \text{(C1a)}$$

$$\Delta J_2 = J_2(r,m,g) - J_2(0,m,g) \ , \quad \text{(C1b)}$$

with the integrals

$$J_\alpha(r,m,g) = \frac{S_{d-1}}{2\pi}\int_0^\infty\int_0^\pi q^{d-1}\sin^{d-2}\theta\, Y_\alpha(\theta,q)\,\mathrm{d}\theta\mathrm{d}q \ , \quad \text{(C2)}$$

with

$$Y_1(\theta,q) = \frac{g\left(r+m+q^2\right)\cos^2\theta}{(r+q^2)\,\Omega} \ , \quad \text{(C3a)}$$

$$Y_2(\theta,q) = \left(\frac{1}{d-1}\right)\frac{2\left(r+q^2\right)\sin^2\theta}{(r+m+q^2)\,\Omega} \ , \quad \text{(C3b)}$$

and Ω from Eq. (A3). These integrals are of the same type as the integrals I_α discussed in Appendix A and they can, in principle, be calculated along the same lines. The essential difference is that in the case of the I_α's we were only interested in the diverging part, while the J_α's have to be calculated exactly to determine the susceptibility χ_{11}^{-1} or the effective exponent γ_{eff}. The series technique presented in Appendix A is not efficient to obtain an exact solution. That is why a different way of calculation is presented below. Only the treatment on J_1 will be discussed in some detail since J_2 can be calculated in the same way. The θ integration is performed using Eq. (A8) and the substitution $x = \cos^2\theta$. It follows that

$$J_1(r,m,g) = \frac{S_{d-1}}{2\pi}\,\frac{\Gamma\left(\frac{d-1}{2}\right)\Gamma\left(\frac{3}{2}\right)}{\Gamma\left(\frac{d}{2}+1\right)}\lim_{\Lambda\to\infty}\int_0^\Lambda q^{d-1}\frac{g\left(r+m+q^2\right)}{\left(r+q^2\right)^2\left(r+m+g+q^2\right)} \times F\left(1,\frac{3}{2};\frac{d}{2}+1;\frac{-gm}{(r+q^2)\left(r+m+g+q^2\right)}\right)\mathrm{d}q \ , \quad \text{(C4)}$$

where $F(a,b;c;z)$ is the hypergeometric function.[52] In four dimensions ($d = 4$), both J_1 and J_2 diverge for an infinite cutoff radius $\Lambda \to \infty$. The quantities ΔJ_α, however, are finite for $\Lambda \to \infty$ and these are the quantities which have to

be calculated to the order ϵ^0 with $\epsilon = 4 - d$. Therefore, within the framework of the ϵ expansion, we can perform the calculation directly at $\epsilon = 0$ or $d = 4$. At $d = 4$, Eq. (C4) can be simplified using the relation[52]

$$F\left(1, \frac{3}{2}; 3; z\right) = \frac{4}{\left[1 + \sqrt{1 - z}\right]^2} \tag{C5}$$

and the substitutions

$$x = q^2 \,, \tag{C6a}$$

$$\mu = \frac{m + g}{2} \,, \qquad \text{and} \qquad \Delta = \frac{m - g}{2} \,, \tag{C6b}$$

$$u = x + r + \mu \,. \tag{C6c}$$

It follows that

$$J_1(r, m, g) = \frac{S_d}{2} g \lim_{x \to \infty} \int_{r+\mu}^{x+r+\mu} \frac{(u - r - \mu)(u + \Delta)}{(u - \mu)^2 (u + \mu)} \left[1 + \sqrt{\frac{u^2 - \Delta^2}{u^2 - \mu^2}}\right]^{-2} \mathrm{d}u \,. \tag{C7}$$

This result is rewritten as

$$J_1(r, m, g) = \frac{S_d}{2m^2 g} \left[L_1(r, m, g) + L_2(r, m, g) - 2 L_3(r, m, g)\right] \,, \tag{C8}$$

with the integrals

$$L_1(r, m, g) = \lim_{x \to \infty} \int_{r+\mu}^{x+r+\mu} (u - r - \mu)(u + \Delta)(u + \mu)\, \mathrm{d}u \,, \tag{C9a}$$

$$L_2(r, m, g) = \lim_{x \to \infty} \int_{r+\mu}^{x+r+\mu} \frac{(u - r - \mu)(u + \Delta)^2 (u - \Delta)}{(u - \mu)} \mathrm{d}u \,, \tag{C9b}$$

$$L_3(r, m, g) = \lim_{x \to \infty} \int_{r+\mu}^{x+r+\mu} (u - r - \mu)(u + \Delta)(u + \mu) \sqrt{\frac{u^2 - \Delta^2}{u^2 - \mu^2}} \mathrm{d}u \,. \tag{C9c}$$

L_1 and L_2 can be calculated straightforwardly, while L_3 is more complicated. It gives rise to the elliptic integrals and can be calculated using Eqs. (1.2.23.2), (1.2.23.4), (1.2.61.12), and (1.2.61.10) of Ref. 62. The lengthy result for ΔJ_1 as defined in Eq. (C1a) will not be given here. After obtaining ΔJ_2 from a similar procedure one can finally calculate γ_{eff} according to Eqs. (53) and (59). One requires the quantities

$$S_\alpha = -\frac{\tau}{2S_d} \frac{\partial}{\partial \tau} \Delta J_\alpha \left(1, \frac{m}{\tau}, \frac{g}{\tau}\right) \,. \tag{C10}$$

The result (62) is obtained after a lengthy but straightforward calculation by using S_0 from Eq. (60) as well.

APPENDIX D: DISCUSSION OF THE ELLIPTIC INTEGRALS

The result (62) for γ_{eff} involves the elliptic integrals of the first and second kinds which are defined as[52]

$$F(\varphi, k) = \int_0^\varphi \frac{1}{\sqrt{1 - k^2 \sin^2 \alpha}} \mathrm{d}\alpha \,, \tag{D1}$$

and

$$E(\varphi, k) = \int_0^\varphi \sqrt{1 - k^2 \sin^2 \alpha}\, \mathrm{d}\alpha \,. \tag{D2}$$

In the case of Eq. (62),

$$k = \frac{a-1}{a+1} , \tag{D3}$$

while φ is given by Eq. (64). In the limit $a \to 0$, the arguments of the elliptic integrals become $k^2 \to 1$ and $\varphi \to \pi/2$. It is obvious from Eq. (D1) that $F(\varphi, k)$ is divergent in this case. It turns out that the divergence is logarithmic and is canceled exactly by the other logarithmic terms of Eq. (62). Consequently, γ_{eff} is finite in the limit $a \to 0$.

To perform an expansion of the elliptic integrals in powers of a and a/y the integral is broken into two parts: the complete elliptic integral $F(\pi/2, k)$ and the small quantity $\delta(\varphi, k) = F(\pi/2, k) - F(\varphi, k)$. To treat the complete elliptic integrals $F(\pi/2, k)$ and $E(\pi/2, k)$ some well-known expansions[61] in powers of $k' = \sqrt{1-k^2}$ are exploited. One finally obtains the result

$$\begin{aligned} F(\varphi, k) = & -\frac{1}{2}\left[1 + a + \frac{1}{4}a^2 + \frac{1}{4}a^3 + O\left(a^4\right)\right] \ln a \\ & + \ln 2 + \frac{1}{2}\ln\left(\frac{y}{y+1}\right) + \frac{1}{4}\left[2\ln\left(\frac{y}{y+1}\right) + 4\ln 2 + \frac{1}{y(y+1)}\right] a \\ & + \frac{1}{32}\left[4\ln\left(\frac{y}{y+1}\right) + 8\ln 2 - \frac{3 - 4y - 10y^2 + 4y^3 + 4y^4}{y^2(y+1)^2}\right] a^2 + O\left(a^2\right) . \end{aligned} \tag{D4}$$

For the expansion of $E(\varphi, k)$ it follows that

$$\begin{aligned} E(\varphi, k) = & \left[-a + \frac{1}{2}a^2 - \frac{3}{4}a^3 + \frac{9}{16}a^4 + O\left(a^5\right)\right] \ln a + 1 + \frac{1}{2}\left[2\ln\left(\frac{y}{y+1}\right) + 4\ln 2 - \frac{1 + 4y + 2y^2}{y(y+1)}\right] a \\ & - \frac{1}{8}\left[4\ln\left(\frac{y}{y+1}\right) + 8\ln 2 - \frac{3 + 16y + 32y^2 + 24y^3 + 6y^4}{y^2(y+1)^2}\right] a^2 \\ & + \frac{1}{16}\left[12\ln\left(\frac{y}{y+1}\right) + 24\ln 2 - \frac{5 + 27y + 65y^2 + 106y^3 + 144y^4 + 65y^5 + 16y^6}{y^3(y+1)^3}\right] a^3 + O\left(a^4\right) . \end{aligned} \tag{D5}$$

---

* On leave from the Institute of Applied Physics, Technical University, 1756 Sofia, Bulgaria.

[1] M. E. Fisher, Rev. Mod. Phys. **46**, 597 (1974).
[2] A. D. Bruce, Adv. Phys. **29**, 111 (1980).
[3] J. C. L. Guillou and J. Zinn-Justin, Phys. Rev. Lett. **39**, 95 (1977).
[4] J. Kötzler, J. Magn. Magn. Mater. **54–57**, 649 (1986).
[5] K. Ried, Y. Millev, and M. Fähnle, in *Trends in Statistical Physics* (Council of Scientific Information, Trivandrum, India, in press).
[6] M. E. Fisher and A. Aharony, Phys. Rev. Lett. **30**, 559 (1973).
[7] A. Aharony and M. E. Fisher, Phys. Rev. B **8**, 3323 (1973).
[8] K. G. Wilson and M. E. Fisher, Phys. Rev. Lett. **28**, 240 (1972).
[9] K. G. Wilson and J. Kogut, Phys. Rep. **12**, 75 (1974).
[10] E. K. Riedel and F. J. Wegner, Z. Phys. **225**, 195 (1969).
[11] M. E. Fisher and P. Pfeuty, Phys. Rev. B **6**, 1889 (1972).
[12] P. Pfeuty, D. Jasnow, and M. E. Fisher, Phys. Rev. B **10**, 2088 (1974).
[13] A. Aharony, Phys. Rev. B **8**, 3358 (1973).
[14] A. Aharony, in *Phase Transitions and Critical Phenomena*, edited by C. Domb and M. S. Green (Academic Press, London, 1976), Vol. 6, pp. 357–424.
[15] A. D. Bruce and A. Aharony, Phys. Rev. B **10**, 2078 (1974).
[16] A. I. Larkin and D. E. Khmel'nitskiĭ, Zh. Eksp. Teor. Fiz. **56**, 2087 (1969) [Sov. Phys. JETP **29**, 1123 (1969)].
[17] A. Aharony, Phys. Lett. **44A**, 313 (1973); Phys. Rev. B **8**, 3363 (1973); **9**, 3946 (1974).
[18] E. Brézin and J. Zinn-Justin, Phys. Rev. B **13**, 251 (1976).
[19] M. E. Fisher, S.-K. Ma, and B. G. Nickel, Phys. Rev. Lett. **29**, 917 (1972).
[20] K. G. Wilson, Phys. Rev. Lett. **28**, 548 (1972).
[21] K. G. Wilson and M. E. Fisher, Phys. Rev. Lett. **28**, 548 (1972).
[22] F. Wegner, Phys. Rev. B **5**, 4529 (1972).
[23] D. R. Nelson and E. Domany, Phys. Rev. B **13**, 236 (1976), [this paper contains some errors; see Ref. 1 of E. Domany *et al., ibid.* **15**, 3493 (1977) for details].
[24] A. D. Bruce and D. J. Wallace, J. Phys. A **9**, 1117 (1976).
[25] E. Domany, D. R. Nelson, and M. E. Fisher, Phys. Rev. B **15**, 3493 (1977).
[26] A. D. Bruce, J. M. Kosterlitz, and D. R. Nelson, J. Phys. C **9**, 825 (1976).
[27] A. D. Bruce, J. Phys. C **10**, 419 (1977).
[28] D. J. Amit and Y. Y. Goldschmidt, Ann. Phys. (N.Y.) **114**, 356 (1978).
[29] J. S. Kouvel and M. E. Fisher, Phys. Rev. **136**, A1626 (1964).
[30] T. Nattermann and S. Trimper, J. Phys. C **9**, 2589 (1976).
[31] E. Frey and F. Schwabl, J. Phys. (Paris) Colloq. **49**, C8-1569 (1988); Phys. Rev. B **43**, 833 (1991).
[32] H. S. Kogon and A. D. Bruce, J. Phys. C **15**, 5729 (1982).
[33] D. Bailin and A. Love, J. Phys. C **10**, 3633 (1977).

[34] E. Frey and F. Schwabl, Phys. Rev. B **42**, 8261 (1990).
[35] C. R. Stephens, J. Magn. Magn. Mater. **104-107**, 297 (1992).
[36] R. Frowein, J. Kötzler, B. Schaub, and H. G. Schuster, Phys. Rev. B **25**, 4905 (1982).
[37] H. Horner, Z. Phys. B **23**, 183 (1976).
[38] K. Ried, Y. Millev, M. Fähnle, and H. Kronmüller, Phys. Lett. A **180**, 370 (1993).
[39] D. Köhler and H. Kronmüller, J. Magn. Magn. Mater. **92**, 344 (1991).
[40] K. Ried, D. Köhler, and H. Kronmüller, J. Magn. Magn. Mater. **116**, 259 (1992).
[41] K. Ried, Y. Millev, M. Fähnle, and H. Kronmüller, Phys. Rev. B **49**, 4315 (1994).
[42] A. D. Bruce, J. Phys. C **7**, 2089 (1974).
[43] T. Nattermann, J. Phys. A **10**, 1757 (1977).
[44] J. Kötzler and G. Eiselt, Phys. Lett. **58A**, 69 (1976).
[45] I. K. Kamilov and K. K. Aliev, Usp. Fiz. Nauk. **140**, 639 (1983) [Sov. Phys. Usp. **26**, 696 (1983)].
[46] K. Ried, H. Gerth, D. Köhler, and H. Kronmüller, J. Magn. Magn. Mater. **109**, 275 (1992).
[47] H. Gerth and H. Kronmüller, J. Magn. Magn. Mater. **130**, 73 (1994).
[48] D. J. Amit, *Field Theory, the Renormalization Group, and Critical Phenomena*, 2nd ed. (World Scientific, Singapore, 1984).
[49] E. Brezin, J. C. L. Guillou, and J. Zinn-Justin, in *Phase Transitions and Critical Phenomena*, edited by C. Domb and M. S. Green (Academic Press, London, 1976), Vol. 6, pp. 125–247.
[50] G. 't Hooft and M. Veltmann, Nucl. Phys. B **44**, 189 (1972).
[51] R. Folk and G. Moser, Phys. Lett. A **120**, 39 (1987).
[52] *Handbook of Mathematical Functions*, edited by M. Abramowitz and I. A. Stegun (Dover, New York, 1965).
[53] M. Fähnle and J. Souletie, J. Phys. C **17**, L469 (1984).
[54] M. Fähnle and J. Souletie, Phys. Rev. B **32**, 3328 (1985).
[55] K. P. Belov, Y. V. Ergin, R. Z. Levitin, and A. V. Ped'ko, Zh. Eksp. Teor. Fiz. **47**, 2080 (1964) [Sov. Phys. JETP **20**, 1397 (1965)].
[56] D. J. W. Geldart, P. Hargraves, N. M. Fujiki, and R. A. Dunlap, Phys. Rev. Lett. **62**, 2728 (1989).
[57] K. K. Aliev, I. K. Kamilov, and A. M. Omarov, Zh. Eksp. Teor. Fiz. **94**, 153 (1988) [Sov. Phys. JETP **67**, 2262 (1988)].
[58] K. H. J. Buschow, Mater. Sci. Rep. **1**, 1 (1986).
[59] M. Seeger, Ph.D. thesis, Stuttgart University, Germany, 1991.
[60] A. R. Chowdhury, G. S. Collins, and C. Hohenemser, Phys. Rev. B **33**, 6231 (1986).
[61] I. M. Ryshik and I. S. Gradstein, *Summen-, Produkt- und Integraltafeln* (VEB Deutscher Verlag der Wissenschaften, Berlin, 1963).
[62] A. P. Prudnikov, J. A. Bryčkov, and O. I. Maričev, *Integraly i Rjadi* (Nauka, Moskau, 1981), Vol. 1.